

**THE EFFECTS OF CHANGES IN LAND USE LAND  
COVER ON THE HYDROLOGICAL RESPONSE IN  
UPPER INDUS BASIN**



By

**AHMAD AMMAR**

**2010-NUST-MS PhD-GIS-21**

**A thesis submitted in partial fulfillment of the requirements for the  
degree of Master of Science in Remote Sensing and GIS**

**Institute of Geographical Information Systems**

**School of Civil and Environmental Engineering**

**National University of Sciences & Technology**

**Islamabad, Pakistan**

**June, 2014**

## **ACADEMIC THESIS: DECLARATION OF AUTHORSHIP**

I, Ahmad Ammar, declare that this thesis and the work presented in it are my own and have been generated by me as the result of my own original research.

### **The Effects of changes in land use land cover on hydrological response in upper Indus basin**

I conform that:

- 1.1** This work was done wholly by me in candidature for an MS research degree at the National University of Sciences and Technology, Islamabad.
- 1.2** Wherever I have consulted the published work of others, it has been clearly attributed.
- 1.3** Wherever I have quoted from the work of others, the source has been always cited. With the exception of such quotations, this thesis is entirely my own.
- 1.4** I have acknowledged all main sources of help.
- 1.5** Where the work of thesis is based on work done by myself jointly with others, I have made clear exactly what was done by others and what I have contributed myself.
- 1.6** None of this work has been published before submission. This work is not plagiarized under the HEC plagiarism policy.

Signed: .....

Date: .....

# **DEDICATION**

**Dedicated to My Parents**

## **ACKNOWLEDGEMENTS**

I would like to thank the following people and organizations whose valuable help and assistance have made the completion of this study possible.

Dr. Muhammad Umar Khan Khattak, my supervisor, for providing generous support to pursue trainings for professional development and for ensuring that I finish the thesis according to the schedule. I am also thankful for his continuous encouragement, perpetual guidance, thoughtful suggestions and constructive criticism during the entire dissertation period. He was a constant source of inspiration and encouragement throughout my research.

I want to give credit to my GEC members for their continuous assistance and guidance on my thesis. Their ideas during data collection, processing and analysis enabled me to refine my work. I would like to thank IGIS management staff especially Mr. Sajid Mahmood for facilitating me throughout my research.

I would like to acknowledge Flood Forecasting Commission Islamabad for providing stream flow data on daily basis from 2000-2010 is highly appreciated. I am also thankful to Mr. Raza Shah from UNESCO, Pakistan for guiding me. This research was possible with the generous research fund provided by NUST.

I am also thankful to all my class fellows, friends, colleagues and family members for their sincere attitude, moral support and prayers which inspired me every moment towards successful completion of my research.

# TABLE OF CONTENTS

ACADEMIC THESIS: DECLARATION OF AUTHORSHIP.....	i
DEDICATION.....	ii
ACKNOWLEDGEMENTS.....	iii
LIST OF FIGURES.....	vii
LIST OF TABLES.....	ix
LIST OF ABBREVIATIONS.....	x
ABSTRACT.....	xi
<b>INTRODUCTION.....</b>	<b>1</b>
1.1 BACKGROUND INFORMATION.....	1
1.2 RATIONALE.....	3
1.3 OBJECTIVES OF THE STUDY.....	4
1.4 SCOPE OF THE WORK.....	4
1.5 STUDY AREA.....	4
1.5.1 Geological Setting.....	7
1.5.2 Geography.....	7
1.5.3 Climate and Precipitation Trends.....	7
1.5.4 Division of Upper Indus Basin.....	8
1.5.5 Tarbela Dam.....	9
<b>LITERATURE REVIEW.....</b>	<b>11</b>
2.1 RUNOFF AND DISCHARGE.....	11
2.2 FLOODS AND TYPES OF FLOODS.....	12
2.2.1 Single storm flood.....	13
2.2.2 Multiple event floods.....	13
2.3 HYDROLOGICAL MODELING.....	13
2.4 CATEGORIES OF HYDROLOGICAL MODELS.....	14
2.5 ROLE OF REMOTE SENSING IN HYDRO MODELING.....	15
2.6 ROLE OF GIS IN HYDROLOGICAL MODELING.....	16
2.7 DISCUSSION OF MODELS.....	16
2.8 HEC-GEOHMS MODEL.....	17
2.9 HEC-HMS MODEL.....	18
2.10 REASON TO CHOOSE HEC-HMS MODEL.....	19
2.11 SCS-CN METHOD.....	20

2.11.1	Hydrological Soil Groups HSG .....	21
2.11.2	CURVE NUMBER CN .....	22
2.11.3	Antecedent moisture condition (AMC) .....	23
2.12	LOSS METHOD FOR HEC-HMS MODEL.....	23
2.13	TRANSFORM METHOD FOR HEC-HMS MODEL.....	24
2.13.1	CN lag Method .....	25
2.14	SENSITIVITY ANALYSIS AND VALIDATION.....	25
2.15	LAND USE LAND COVER CHANGE DETECTION.....	25
2.16	SATELLITE IMAGE CLASSIFICATION.....	26
2.17	ACCURACY ASSESSMENT OF SATELLITE IMAGE CLASSIFICATION 27	
2.17.1	Error Matrix.....	27
2.17.2	Kappa Coefficient.....	28
2.18	PRECIPITATION MEASUREMENT .....	29
2.19	SATELLITE PRECIPITATION (TRMM) DATA.....	30
2.19.1	Precipitation radar.....	31
2.19.2	Pakistan rainfall pattern .....	31
2.20	ADVANTAGES AND DISADVANTAGES OF SATELLITE PRECIPITATION.....	32
<b>MATERIALS AND METHODS .....</b>		<b>34</b>
3.1	DATASETS FOR STUDY .....	34
3.1.1	Landsat Satellite images .....	34
3.1.2	Soil data and HSG map.....	34
3.1.3	Topographic data .....	35
3.1.4	Hydro-Meteorological data.....	35
3.1.5	Remote Sensing (TRMM) Precipitation Data.....	36
3.2	DATA PROCESSING .....	36
3.2.1	Landsat image processing.....	36
3.2.2	Generation of Curve Numbers.....	37
3.2.3	Processing of Precipitation Data.....	40
3.3	ANALYTICAL FRAMEWORK.....	40
3.4	HEC-GEO HMS PROCESSING .....	42
3.4.1	DEM Hydrological Processing .....	42
3.4.2	Generating a Project.....	42
3.4.3	Threshold Value for The Project.....	43
3.4.4	Basin Processing .....	43
3.4.5	Longest Flow Path Calculation.....	43

3.4.6	Basin Centroid and Centroidal Flow Path .....	43
3.4.7	Sub-Basin Parameters through Raster .....	44
3.4.8	CN lag Method.....	44
3.4.9	Generation of Files for HEC-HMS .....	44
3.5	HEC-HMS MODEL SETUP .....	45
3.5.1	Basin Model .....	45
3.5.2	Meteorological Model.....	46
3.5.3	Control Specification .....	46
3.6	MODEL CALIBRATION AND VALIDATION .....	47
3.7	STATISTICAL TEST .....	48
3.7.1	Correlation Coefficient .....	48
3.7.2	The Relative Bias (BIAS) .....	49
3.7.3	Nash–Sutcliffe Coefficient of Efficiency.....	49
	<b>RESULTS AND DISCUSSIONS .....</b>	<b>51</b>
4.1	LULC CHANGE ANALYSIS .....	51
4.2	ACCURACY ASSESSMENT FOR 2010 LANDSAT IMAGE CLASSIFICATION .....	53
4.3	LULC CHANGE.....	53
4.4	CALIBRATION AND VALIDATION OF HEC-HMS MODEL.....	56
4.5	HEC-HMS MODEL RESULTS .....	56
4.5.1	Statistical Analysis of Results.....	59
4.6	SENSITIVITY ANALYSIS OF HEC-HMS.....	60
4.6.1	Sensitivity Analysis for Curve Number.....	61
4.6.2	Sensitivity Analysis for Initial Abstraction.....	61
4.7	SENSITIVITY ANALYSIS FOR LULC .....	63
4.8	MANSEHRA CITY SUB-WATERSHED ANALYSIS.....	64
	<b>CONCLUSIONS AND RECOMMENDATIONS.....</b>	<b>68</b>
5.1	CONCLUSION .....	68
5.2	RECOMMENDATIONS .....	70
	<b>REFERENCES.....</b>	<b>71</b>

## LIST OF FIGURES

Figure 1.1. Estimates of worldwide flood damage distribution (in million \$) from 1900 to 2012 (chart reproduced from Asian Development Bank report on Indus Basin floods 2013).	2
Figure 1.2. Area of interest (study area) in the upper reaches of the Indus basin from Bisham Qila in the north to Tarbela reservoir in the south located in the north western part of Pakistan. Map shows the topographic features as depicted in the digital elevation model (DEM) of SRTM (Shuttle Radar Topographic Mission) at 90 m horizontal resolution for the study area. The map also shows Indus River and district administrative boundaries in and around the study area.	6
Figure 1.3. Map showing mean annual rainfall distribution in Pakistan. The study area lies in the region showing the higher value of annual rainfall in the north western Pakistan (source: PMD-2010)	10
Figure 2.1. HEC-HMS model interface. There are 3 main components. 1) Watershed explorer, showing the Basin model, meteorological model and control specification; 2) Component editor, to edit the values of watershed components and; 3) Desktop, showing the watershed and its components like sub-basins, reaches, sinks etc.	19
Figure 3.2. Curve Number Raster generated from LULC and Soil data. The dark shades represent higher value of CN and thus higher runoff potential areas while the brighter colors represent lower runoff potential areas.	39
Figure 3.3. Overall methodology for carrying out the research. It has four major parts; 1) DEM processing, which was done in HEC-GeoHMS extension of ArcGIS; 2) Soil map was processed to extract Hydrological Soil Groups for the study area; 3) precipitation data was downloaded and converted to input in the model HEC-HMS; 4) satellite images were classified to produce LULC maps. All the data was given in the model and after calibration and optimization, valid results were produced.	41
Figure 4.1. LULC map of 2000 and 2010 produced after supervised image classification of the Landsat satellite images. The LULC classes include soil, forest water, grass and built-up area.	52
Figure 4.2. Bar graph showing comparison of change in each LULC class from 2000 to 2010	55
Figure 4.3. Bar graph showing comparison of observed and simulated discharge for rainfall event days selected for year 2000 and 2010 (15 July to 15 September)	57
Figure 4.4. Comparison of simulated discharge for 2000 generated by the model after calibration, plotted versus the observed discharge values at Tarbela outlet	58
Figure 4.5. Comparison of simulated discharge for 2010 generated by the model after calibration, plotted versus the observed discharge values at Tarbela outlet	58
Figure 4.6. Scatter plot for 3 months (July-September) with regression line between observed and simulated discharge for 2000 and 2010	59
Figure 4.7. Sensitivity index for the parameters showing the more sensitive parameter of CN and less sensitive parameter of initial abstraction.	60
Figure 4.8. Line graph for sensitivity analysis of CN parameter	62
Figure 4.9. Line graph for sensitivity analysis of LULC scenarios of 2000 and 2010. Graph shows that discharge simulated with 2010 LULC is slightly higher than the discharge generated with 2000 LULC scenario. But the difference is negligible overall.	63

Figure 4.10. LULC of metropolitan sub-watershed in Mansehra District of KP province in Pakistan with a distinct proportion off built-up class in it. .... 65

Figure 4.11. Graph showing the difference in percentage increase of discharge for whole Tarbela watershed with less than 1% built area and sub-watershed in Mansehra with about 10% built-up area. .... 67

## LIST OF TABLES

Table 2.1. Classification of hydrological soil groups by USDA-NRCS 2007.....	22
Table 2.2. Soil AMC for different ranges of cumulative rainfall in dormant and rainy season .....	23
Table 3.1. Dominant soil types and Hydrological Soil Group in the study area obtained from World Digital Soil Map (WDSM). ....	35
Table 3.2. 48 sub-basins were generated by HEC-GeoHMS . Sub-basin wise elements details of some of those sub-basins are given in the table. Unit hydrograph was selected as Transform method, SCS-CN as loss method and CNlag as the lag method to generate these elements. ....	46
Table 4.1. Error matrix generated for accuracy assessment. The diagonal elements show the accurately classified pixel values. Table also show the user accuracy and producer accuracy .....	54
Table 4.2. LULC types and corresponding area for the year 2000 and 2010. Percentage increase or decrease in area is also calculated. ....	55
Table 4.3. Observed and model simulated discharge for random days of 2000 and 2010 .....	57
Table 4.4. Statistical analysis results .....	59
Table 4.5. Sensitivity analysis values for curve number parameter. The corresponding discharge values for each CN are given along with the observed discharge at Tarbela gauge.....	62
Table 4.6. LULC change of Mansehra subwatershed for the year 2000 and 2010.....	65
Table 4.7. Comparing the percentage increase in discharge values for whole Tarbela watershed and sub-watershed at Mansehra.....	67

## LIST OF ABBREVIATIONS

Notation	Representation
ASCII	American Standard for Computer and Information Interchang
BIAS	Relative Bias
BIN	Binary
CC	Correlation Coefficient
CN	Curve Number
DEM	Digital Elevation Model
FAO	Food And Agriculture Organization
FFC	Flood Forecasting Commission
GIS	Geographical Information Systems
HEC-HMS	Hydrologic Engineering Center-Hydrologic Modeling System
HSG	Hydrologic Soil Group
KP	Khyber Pakhtunkhwa
LULC	Land Use Land Cover
NASA	National Aeronautics and Space Administration
NASDA	National Space Development Agency
PMD	Pakistan Meteorological Department
PR	Precipitation Radar
SCS	Soil Conservation Service
SRTM	Shuttle Radar Topography Mission
TRMM	Tropical Rainfall Measuring Mission
UIB	Upper Indus Basin
USGS	United States Geological Survey
WAPDA	Water And Power Development Authority

## **ABSTRACT**

Empirically based lumped hydrologic models have an extensive track record of use for various watershed managements and flood related studies. This study focuses on the impacts of land use land cover change for a 10 year period on the stream discharge in a sub-watershed of Indus River using lumped model HEC-HMS. The Indus above Tarbela region acts as a source of main flood events in the middle and lower portions of Indus basin because of the amount of rainfall and geomorphological setting of the region. The discharge pattern of the region is influenced by the LULC associated with it. In this study the Landsat TM images were used to conduct LULC analysis of the sub-watershed. Satellite daily precipitation estimation of Tropical Rainfall Measuring Mission (TRMM) data was used as input rainfall. The input variables for model building in HEC-HMS were calculated based on the Digital Elevation Model, Land use Land cover, soil and precipitation data which was collected and pre-processed in HEC-GeoHMS. SCS-CN was used as transform model, SCS unit hydrograph method was used as loss model and Muskingum method was used for flow routing. For discharge simulation years 2000 and 2010 were selected. HEC-HMS was calibrated for the year 2000 and then validated for 2010.

The model calibration statistics for  $n = 90$  (monsoon season during July, August and September) are correlation coefficient = 0.96, relative Bias = 2.5% and Nash-Sutcliffe coefficient of efficiency (NSCE) = 0.89. The model validation statistics are CC = 0.95, Bias = -3.7% and NSCE = 0.94. The model results confirm the results of the LULC change analysis using Landsat TM images that in 10 years the impact of LULC change on discharge has been negligible in the study area overall. This is possibly due to the fact that the proportion of the built-up area in the sub-watershed, which is the main causative factor of change in discharge, is less than 1% of the total

area. This conclusion was further supported by the LULC change analysis conducted on a local scale metropolitan district of Mansehra, where the impact of development was found significant in the built up area and corresponding discharge. The analysis was done on Mansehra city sub-watershed with an area of about 16 km<sup>2</sup>. Built up area in this sub-watershed increased from 8.2% in 2000 to 13.76% in 2010, whereas the corresponding river discharge increased by 33.61% from year 2000 to 2010, proving strong positive correlation on a local scale between the LULC and the river discharge. The rainy days of more than 15 mm rain were considered to generate river discharge and the change in percentage was averaged. The results showed that with an increase of 40% built-up area in the city from 2000 to 2010 the discharge values increased about 33 percent, indicating the impact of LULC change on discharge value.

## **INTRODUCTION**

### **1.1 BACKGROUND INFORMATION**

Flood is the most devastating disaster among all the natural disasters because of its extent and recurrence. Floods are natural phenomena associated with the slopes, rivers and channels. Rivers are the largest source of fresh water on earth. So, human societies settle and flourish along the banks of rivers more than anywhere else on the globe. Because of large population near the rivers, the life loss and financial loss due to floods is also large. Reports show that only in the year 2010, more than 178 million people were directly affected by the floods around the world and that flood events across the globe are responsible for more than one third economic losses of the world (Abhas et al., 2012). A comparison of the economic losses among different continents shows that Asia is the most affected region with floods (Figure 1.1).

Among several reasons which influence the flooding phenomenon to happen, poor management and unplanned human constructions along the river banks is one of the most important one. Especially in a developing country like Pakistan where population growth is on the higher side, people need more space for settlements as well as more resources to build them. So, the rate of urbanization and deforestation adds to the main factors which increase the severity as well as number of flood events.

In the Indus Basin, flood-causing factor includes monsoonal rain which is most important one, followed by the size, shape, and land-use of the catchments, and by the transferring capacity of the streams associated with Indus. The monsoon rains fall from July to September, and are generally intense and widespread caused by the weather systems originating in the Indian Ocean and the Arabian Sea. The rain pattern is more

complexed by the interference of other weather systems, such as westerlies originating in the Mediterranean Sea, some local convection depressions and some orographic low pressure systems.

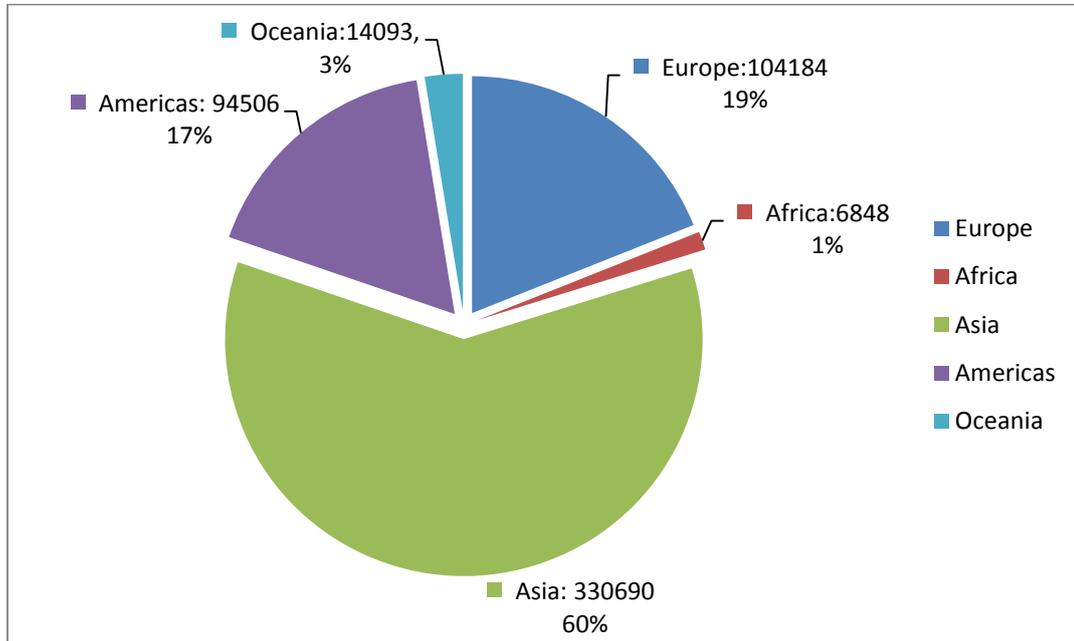


Figure 1.1. Estimates of worldwide flood damage distribution (in million \$) from 1900 to 2012 (chart reproduced from Asian Development Bank report on Indus Basin floods 2013).

Flood estimation due to precipitation in watersheds is a very important applied analysis in hydrology. In reality a watershed system is a complex hydrological system requiring lots of data for understanding it. Hydro-modeling represents the hydrological phenomenon happening in a watershed in a simple way through equations. The purpose of hydro-modeling is to understand the natural system to increase human welfare and to manage of water resources. Understanding watersheds' hydrologic behavior in a data deprived scenario on one hand and complexity of hydrological systems on the other hand causes inevitable use of rainfall-runoff simulation models. To study these rainfall-runoff simulations becomes necessary because of lack of data available.

Today we have many tools available to model and visualize rainfall to flood dynamics. Some of these tools are available using Geographic Information Systems (GIS). GIS can be used to merge rainfall data with stream flow values to model and visualize falling precipitation, runoff, and rising streams. Increasingly, GIS are incorporating time elements into their analytical capacities. These time elements known as spatio-temporal data enhance modeling of real world phenomena. Incorporating spatial-temporal data into various aspects of watershed management is a simple way to analyze stream flow data and form a basic flood model. Because of the fact that hydrological as well as geomorphological characteristics vary spatially, the use of GIS facility has gained a lot of attention in the recent times, whereby analysis at different scales can be done and all the variations can be taken into account (Melesse and Shih, 2002).

## **1.2 RATIONALE**

The Indus River basin in the Tarbela region acts as a source of the main flood events in the lower portions. This region receives the highest amount of rainfall in the whole country. Indus watershed above Tarbela reservoir is a mountainous region having a good proportion of forest cover. Human population is sparse and mainly distributed on the mountain slopes.

The purpose of this study is to analyze the hydrological characteristics of the study area and to evaluate the impact of change in the land use land cover on increasing the severity of the flood event. To study the phenomenon responsible for any change in discharge pattern from precipitation is important for flood management. Spatial hydrology can be one of the best ways to perform analysis on the area with difficult

access. So Satellite remote sensing data and hydrological model HEC-HMS is used to calculate the discharge generated in the region

### **1.3 OBJECTIVES OF THE STUDY**

- To carry out the land use land cover change analysis from 2000 to 2010.
- To calibrate and validate the hydrological model HEC-HMS for the Indus River reach from Bisham Qila to Tarbela.
- To find the effects of changes in land use land cover on the hydrological discharge in the catchment.

### **1.4 SCOPE OF THE WORK**

- Reviewing and searching literature on hydrological modeling and characteristics to establish a reliable relationship between rainfall-runoff modeling and land use land cover change for the Tarbela catchment.
- Obtain the related rainfall and discharge data from different Departments and remote sensing data from internet.
- Producing land use map and identifying the change in the land use within a fixed time domain in the catchment area.
- Selecting a suitable model and then calibrating and validating the model for calculation of discharge in the catchment
- Relating the change in land use land cover change with the discharge pattern of the catchment.

### **1.5 STUDY AREA**

Pakistan is an agricultural country and its economy relies on the agricultural productions. To get maximum crop yields, Pakistan depends on its water assets, 50%

of those water comes from the surface water in the rivers and streams. The surface water resources of Pakistan include a large network of rivers, mostly received out of a huge glaciological complex housed at 5000 m above mean sea level in the Himalayan-Karakoram- Hindu Kush mountain belt. These rivers and their tributaries serve as the most important part of the country's irrigation system.

The 2737 km long Indus river drains the largest basin in Pakistan and together with its tributary system caters for nearly 90% of the country's agricultural water requirements. The northern Indus basin consists of many rivers and streams. The Indus River is the main river in along with a tributary network of streams which flows throughout the year including the Kabul, Swat, Chitral, Kunhar, Panjkora, Kurram, Gomal and Haro. Together these streams cover most part of the drainage basin of north Pakistan.

There are two distinct portions of Indus above Tarbela region. The larger portion consists of snow covered mountains and glaciers with permanent snow cover. This portion has an area of about 158,000 km<sup>2</sup> and is about 960 km long, 160 km wide. The smaller portion which is about 10000 km<sup>2</sup> is immediate upstream portion to Tarbela reservoir. This portion receives highest amount of monsoonal rainfall and the runoff in this area highly depends on the amount of rainfall (WAPDA, 2001).

The study area is located in KPK province of Pakistan. It starts from the Terbela dam reservoir and ends at Besham station. It is located between latitude 34° and 35° degrees and longitude 72° and 73° degree as shown in figure 1.2.

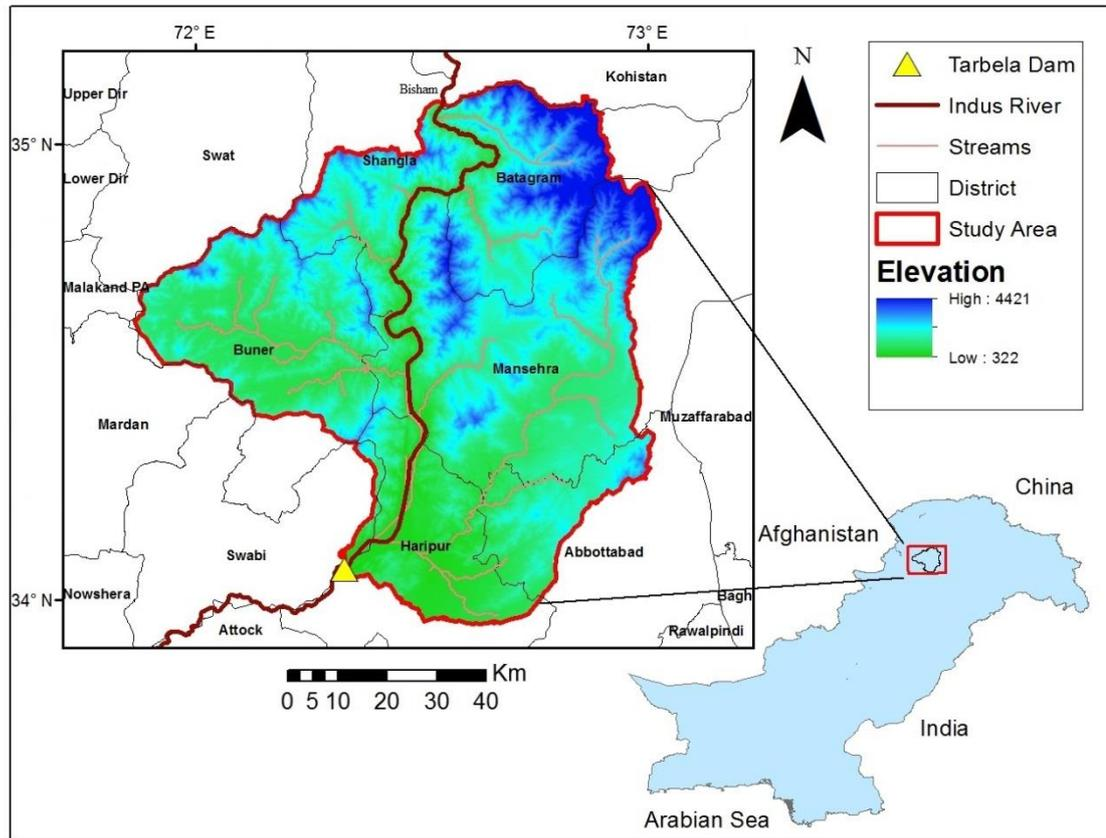


Figure 1.2. Area of interest (study area) in the upper reaches of the Indus basin from Bisham Qila in the north to Tarbela reservoir in the south located in the north western part of Pakistan. Map shows the topographic features as depicted in the digital elevation model (DEM) of SRTM (Shuttle Radar Topographic Mission) at 90 m horizontal resolution for the study area. The map also shows Indus River and district administrative boundaries in and around the study area.

### **1.5.1 Geological Setting**

About 45-50 million years ago, the collision between Indian and Asian plates resulted in the rapid uplift of the Himalayas, Karakoram and Hindukush ranges around the northern and northwestern rim of the Indian plate. The tectonic activity has continued ever since and at least three major phases of uplift and denudation have been completed till Quaternary. Subsequently, the north Pakistan has attained rugged topography and steep relief as is evident from the five peaks of greater than 8000 m and the sixty eight peaks of greater than 7000 meter altitude in a small region. In KPK the more northerly districts of Shangla, Kohistan, Chitral, Dir, Hazara and Swat are largely mountainous.

### **1.5.2 Geography**

The Indus River rises on the Tibetan Plateau and after passing through Baltistan and Gilgit Agencies enters the Khyber Pukhtunkhwa province through Kohistan district. Near Tarbela, the Indus is dammed for flood regulation and electricity production. Upstream Tarbela, the major tributaries of the Indus include Shyok, Shigar, Zaskar, Gilgit, Hunza, Astore and Tangir rivers. The total drainage area of the Indus River just upstream of Tarbela is 162,000 km<sup>2</sup>, and average annual flow at Beesham Qila is 2350 cumec. Downstream of Tarbela reservoir, the Indus River continues its journey through the remaining part of the KP province and enters Punjab near D.I.Khan. In between Tarbela and D.I. Khan, the Indus is joined by the Kabul, Soan, Kurram and Gomal rivers (Rehman, 1997).

### **1.5.3 Climate and Precipitation Trends**

There are two principle sources of precipitation, westerly disturbances from the Mediterranean region and monsoons from the Indian Ocean (Bay of Bengal) and the

Arabian Sea. Climate and topography have a great influence on the timing and magnitude of flows in the river Indus. Indus River flows are composed primarily of water from snow and ice melt, while monsoonal rains may be important in the more southerly basin. The importance of these three main sources varies through time.

Incoming river discharge to Tarbela reservoir is measured at an upstream gauging station of Besham Qila which is situated approximately 80 km north of Tarbela. The mean annual flow at Besham Qila is 2410 m<sup>3</sup>/sec (i.e. 370 mm of water depth equivalent) as calculated in the study conducted by Tahir (2011) from the flow records of 1969–2008 (data provided by the Surface Water Hydrology Project, SWHP). An average annual precipitation of approximately 400 mm is estimated in this study from available data records of different climate stations in Upper Indus Basin (UIB). These precipitation records are available only below 4700 m elevation and almost 50% of UIB area is above this elevation where the maximum snow accumulation occurs. The altitude within the basin ranges from 455 m to 8611 m, (with 8611 m corresponding to the K2 peak — 2nd highest summit on the earth) and as a result the climate varies greatly within the basin (Tahir, 2011).

#### **1.5.4 Division of Upper Indus Basin**

Archer (2003) suggested that UIB can be divided into three hydrological regimes: a) high altitude catchments (e.g. Hunza and Shyok) with summer runoff derived mainly from the snow and glacier melt with concurrent energy input in the form of temperature; b) middle altitude catchments situated at the extreme west of Himalaya (e.g. Astore) where the summer runoff is defined by preceding winter precipitation; and c) low altitude (foothill) catchments that have a runoff regime controlled by the current winter or summer rainfall (Besham to Tarbela region).

Stream flow in the Upper Indus Basin can be categorized in two portions. The lower portion has higher value of stream flow due to rainfall-runoff while the upper portion has lower value of stream flow which is due to just glacier-melt (Ali and Boer, 2007; Archer, 2003). Glacier melt runoff is of more importance as it continues in the entire year providing more than 60% of yearly flow in the river Indus. This snow melt water comes from very high glaciers of Himalaya and Hindu Kush region (Bookhagen and Burbank, 2010).

### **1.5.5 Tarbela Dam**

WAPDA has been monitoring the discharge and sediment load of the Indus River System at various stations since 1962 and publishing the subsequent reports more or less at regular intervals (Rahman, 1997). After the distribution of rivers between Pakistan and India in 1960, the need of regulating the waters of Indus River System was badly required. This led in 1974 to the construction of the world's largest earth-fill dam, the Tarbela dam on the River Indus. Tarbela is the first controlling storage on the River Indus and much of the annual Upper Indus River influx to Tarbela reservoir comes from the snow and glacier melt in Hindukush-Karakoram-Himalaya (HKH) ranges. This water in the reservoir is then supplied downstream to the irrigated lands through a network of barrages, canals and small watercourses (Tahir et al., 2011).

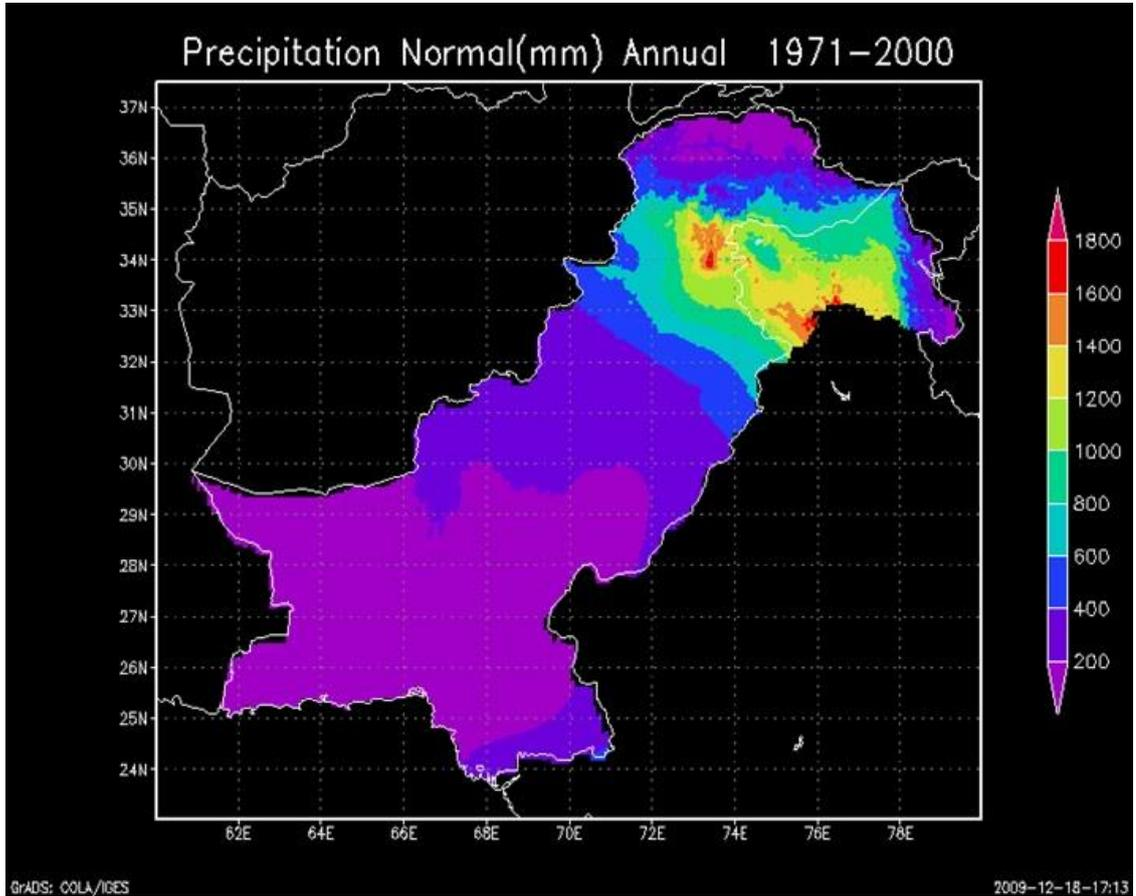


Figure 1.3. Map showing mean annual rainfall distribution in Pakistan. The study area lies in the region showing the higher value of annual rainfall in the north western Pakistan (source: PMD-2010)

## **LITERATURE REVIEW**

### **2.1 RUNOFF AND DISCHARGE**

The hydrological cycle is normally treated as a system that graphically or mathematically represents the movement of water from the oceans to the atmosphere, to land and then back to the oceans through the process of evapotranspiration ET, precipitation P, infiltration I, storage S, base flow and runoff Q. A hydrologic system can be defined as a structure (surface or subsurface), surrounded by a boundary, that accepts water and other inputs, operates on them internally and produces outputs. The basic relations of physical hydrology for this system are derived from fundamental laws of physics in the form of conservation of mass which can be mathematically represented as:

$$P(t) - Q(t) - I(t) - ET(t) - \frac{dS}{dt} = 0$$

In hydrological system, the main parameter entering the system is precipitation which can be termed as a gain for the system. Other parameters entering the system include exfiltration and snowmelt water. The losses, on the other hand, or the parameter leaving the system includes the evapotranspiration, infiltration, storage and runoff.

In hydrology the terms runoff and discharge are among the most important one. Runoff or more specifically surface runoff is the amount of water which flows across the land surface from high elevated land to low elevated land and then it drains into stream or river. The generation of runoff includes a series of events; primarily, the rainfall intensity must exceed the infiltration capacity of the soil and the total losses in evapotranspiration. Initially all of precipitation falling on the surface is infiltrated in the

soil until its saturation. If precipitation keeps on pouring, the infiltration capacity of the soil reduces as the soil gets saturated, after a certain period of time a very small portion of water infiltrates and the remaining water causes surface runoff, a thin water layer formed after the infiltration capacity reaches certain value begins to move downslope due to gravity. Some water accumulates in the depressions. The accumulated water in depressions and the extra water from evapotranspiration and infiltration moves into convergent channels to ultimately form streams and rivers.

Stream discharge represents the quantity of water which flows through a stream during a given period of time. The unit for discharge normally used is cubic meters per second ( $\text{m}^3/\text{sec}$  or cumec). To know the value of discharge for the watershed is very important in conducting flood management.

## **2.2 FLOODS AND TYPES OF FLOODS**

A flood phenomenon happens when the excess volume of water overflows the confinement made, and covers the area of land that is usually dry. Floods in the mountainous areas are generally divided into two categories i.e. flash floods and riverine floods. Flash floods occur due to heavy precipitation for a very short period of time (few hours). The areal inundations are usually very small such as a town or parts of a city. Flash floods can happen in such areas where the rainfall has been low for a long time but a sudden burst of cloud happens and generates flash floods. Riverine flood on the other hand is associated with repeated precipitation events over a larger area and over larger time duration, from few hours to several days. As a result of these events the river overflows from the embankments and large area is inundated with water. Riverine flood can occur well after the precipitation event.

### **2.2.1 Single storm flood**

This type of event is common in mountainous areas along the major river channels. But such events are rare and cause local destructions only. Such high peaks are seen when intensive monsoon rainfall occurs within a day or a single event especially in July, August and September.

### **2.2.2 Multiple event floods**

Due to bad weather or several close storm events, this type of flood occurs. It is a common event in the Indus basin during monsoonal season in Pakistan. In such scenario after a strong rainfall event in the area, second and onward events occur with less time span, almost total amount of precipitation converts to runoff and comes to the channel due to less or no initial loss in the watershed. An example of such event is the precipitation occurred in the last week of July, 2010 which caused the heaviest flood in the region ever recorded.

## **2.3 HYDROLOGICAL MODELING**

Model is basically a representation of reality. Modeling of phenomenon and real happening is always a 'miniature' or the functions of a group of mathematical equations. These equations are not sufficient to represent the total complexity of real world; rather they show the simplification (Karssenber, 2002; Van Loon and Jakob, 2005). Models give more generalized view of basin hydraulics of the real world. With passing time, more advanced capable, multi activities; efficient models are coming continuously and are improving the work status as per requirement. Computer models can handle huge amount of data sets for large drainage networks with a limited time and cost. With advancement in GIS technologies and easy user interface the modeling has become more and more user friendly. Visualization of input and output with

different dimension is possible here and the input error can be corrected and updated continuously in GIS layers. The effective modeling depends upon experience and selection of appropriate model. It is not a replacement of fieldwork which may help to make a better outcome. All models cannot operate or give appropriate result in various spatiotemporal environments though they are made for same purpose.

Modeling is actually making the replica for the actual natural event happening on ground. When we model a natural system, it helps us knowing the system in a better way and this knowledge helps in increasing human welfare and to protect the environment and eco system as well as for planning and management of the watershed (Maity, 2009).

## **2.4 CATEGORIES OF HYDROLOGICAL MODELS**

**Event and continuous model:** An event model simulates single event of precipitation which could be for a few hours or up to several days whereas a continuous model simulates longer period including the time when event occurs and the time when there is no event.

**Lumped or distributed models:** In lumped model the spatial variations are ignored while in distributed model the spatial variation at basin level or pixel level is considered.

**Empirical or conceptual models:** An empirical model is the one which is based on the observations for inputs and outputs whereas the conceptual model has a predefined knowledge based mathematical model having specific processes as input to get an output.

**Deterministic or stochastic models:** Deterministic models are the one in which all the processes, inputs and parameters are known with certainty. If the model describes the random variation in the prediction of output it will be called as stochastic.

Considering the above four categories, the HEC-HMS model is primarily an event based, deterministic and lumped model having both empirical and conceptual variety of modeling in it.

## **2.5 ROLE OF REMOTE SENSING IN HYDRO MODELING**

The never ending process of water cycle through the earth and atmosphere and its forecasting, evaluation, assessment, management is very hard and time taking through conventional methods. Hydrological modeling needs more precise field measured data about several hydrological and basin parameters. There are several issues to collect sufficient data from the field for time, space, economy and security limitations. Remote sensing images help to produce huge information in temporal and spatial domain with different resolutions.

The satellites like GOES, INSAT, TRMM, NOAA etc. are used for cloud types, cloud top temperatures helps indirectly to predict rainfalls with the help of ground network of rain gauge measurements and some relevant developed algorithms. Other satellite data like that of MODIS or Landsat helps in classifying the areas which are physical inaccessible.

The very crucial key variables for the model are extracted without point measurement from remote sensing data with different spectral and spatial resolution. It provides the cost effective synoptic view of different spatial entities that help to create thematic maps of natural and manmade resources like elevation, channel area, surface

water, land use/land cover, soil moisture, vegetation, snow cover, evaporation etc. and their temporal changes.

## **2.6 ROLE OF GIS IN HYDROLOGICAL MODELING**

The subject of modeling is growingly undertaking the integration of spatial and non-spatial information together. Modeling is increasingly used for water quality assessment, water supply, hazard related study, basin management and planning. Geographical information system (GIS) makes the large amount spatial data possible to store, retrieve, correction or manage the complex problem first. Then it helps to analyze the required GIS input for predetermined output layers for different purpose. The geomorphology, land cover, cross section etc. can be seen in different dimension, layers and corrected as requires. In most of the cases remote sensing data are indirectly used for hydrological modeling. So, GIS are obvious to integrate the user and the computer to provide spatial information which helps according to the needs.

## **2.7 DISCUSSION OF MODELS**

A number of hydrologic models have been developed which estimate the peak discharges and the runoff hydrograph for a given rainfall distribution. The applicability and performance of these hydrological models depends on factors such as mathematical representation of processes occurring, structural complexity of the model, and reliability of the model predictions for the available data, geographic location, climatic conditions, and area of interest, physiographic characteristics, computational skill level, Cost and others.

The choice of methods for estimation of peak discharge depends on the data requirements and data availability. Among the different approaches, GIS based

hydrological model system is increasingly becoming major useful tool because of its capability to handle the spatial variation of hydrological and physiographic inputs of the watershed. Several models, which either are embedded in the GIS environment or have capability of importing the GIS derived spatial and temporal attributes, have been developed. One of which is the United States Army Corps of Engineers HEC-HMS (the Hydrologic Engineering centers Hydrological Modeling System). The program simulates the natural and controlled processes of runoff generated by precipitation and routing through watershed processes (USACE, 2000).

## **2.8 HEC-GEOHMS MODEL**

A basin can be more accurately represented by incorporating precipitation and other spatial data in a hydrological model on grid level. HEC-GeoHMS can develop some input files that can be incorporated in lumped model as well as in distributed basin models. Multiple parameters are generated by HEC-GeoHMS model such as grid parameter file, a distributed basin model, lumped basin model, and a background map file, these files are used as input in HEC-HMS for further hydrologic modeling. Hydrologic parameters are estimated in HEC-GeoHMS by formation of attribute tables of each parameter that measures physical characteristics of streams and watersheds in form of shape files. Filling of Dem sinks, Flow direction, flow accumulation, stream definition, stream segmentation, watershed delineation, watershed polygon processing, stream segment processing, watershed aggregation are performed in terrain processing that is the first step in HEC-GeoHMS model next basin processing is done by calculating watershed characteristics, and hydrologic parameter estimation are performed. To develop a catchment that contain an outlet of all the sub basins different sub basins that are generated in HEC-GeoHMS are then merged and aggregated into a

common catchments, finally the results of meteorological model and basin model are exported to HEC-HMS for hydrological modeling a system.

## **2.9 HEC-HMS MODEL**

HEC-HMS is developed by Hydrologic Engineering Center (HEC) of United States Army Corps of Engineers (USACE) and it's a comprehensive hydrologic model. The main function of the model is to analyze precipitation and runoff process in a dendritic type of watershed. Problems in a wide range of geographic areas can be solved using this model because it provides a multiple possible solutions. These include flood hydrology, large river basin water supply, and small urban and natural watershed runoff. Hydrographs that are generated by HEC-HMS can be easily incorporated as input to other models for many other studies of water availability such as flow forecasting , reservoir spillway design, flood plain regulation, future urbanization impact, urban drainage, floodplain regulation, flood damage reduction, , wetlands hydrology (HEC, 2006b). For the simulation of hydrological balance in a watershed components that are generated in HEC-HMS are used as input. These components are basin models, meteorological models, control specifications, and input data. Precipitation values that are given as input in meteorological model are then given to basin model that simulates the rainfall and runoff process in whole watershed. Time period of the model and its time steps are defined in the Control specification in each simulation run. In basin and meteorological models input data components, such as time-series data, paired data, and gridded data are given or requires as parameter and boundary conditions. The following figure shows the main component of the model to be used in this particular study.

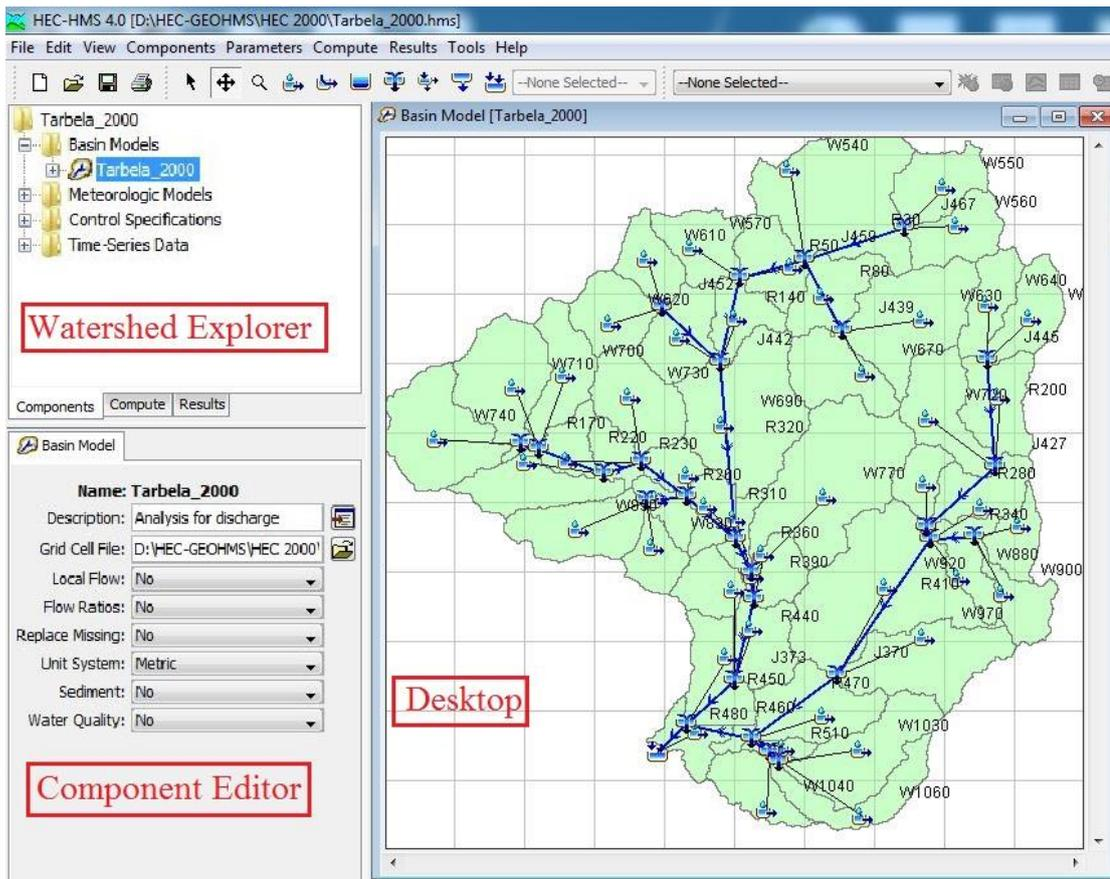


Figure 2.1. HEC-HMS model interface. There are 3 main components. 1) Watershed explorer, showing the Basin model, meteorological model and control specification; 2) Component editor, to edit the values of watershed components and; 3) Desktop, showing the watershed and its components like sub-basins, reaches, sinks etc.

## 2.10 REASON TO CHOOSE HEC-HMS MODEL

The main reasons for the selection of HEC-HMS hydrological model is that the model is physically based, spatially distributed and it belongs to public domain. Different types of hydrological models are being used depending upon the purpose throughout the world. HEC-HMS is a freeware and familiar model for hydrological simulation (Kurothe et al., 2001a). HEC-HMS is suitable for dendritic drainage pattern and it can include various parameters (HEC-HMS Reference Manual, 2000).

HEC-HMS model uses different methods for the simulations of infiltration losses, transforming precipitation excess, estimation of base flow and channel routing. The user can choose a suitable combination of models depending on the availability of

data; the purpose of modeling and the required spatial and temporal scales. It has been used in wide geographical area including climate change studies. Bashar and Zaki (2005) have applied this model for the whole Upper Blue Nile Basin and they have found good performance.

More accurate datasets are needed for acceptable results from the model. So, the intensive field studies for reference, high resolution satellite data for physiography and LULC, sufficient observed gauge and hydro-meteorological datasets are necessary to run and validation of the model (Maidment, 1993; Wilson, 1996).

## **2.11 SCS-CN METHOD**

In HEC-HMS model there is extensive use of SCS methods to define the losses and transformation of rainfall to runoff. Dilip Kumar (2009) and Abayneh Alemu (2011) simulated discharge through HEC-HMS model using SCS method and found high correlation between simulated and observed discharge. The SCS curve number method is a simple method used on large scale for determination of the approximate runoff value corresponding to a certain rainfall quantity in a certain area. The SCS Curve number method only forecasts the quantity of runoff formed in any point of the catchment but does not model the flow routing or the distribution of runoff through time. Because of this reason the requirements of the method are quite low, only the rainfall depth and an empirical parameter named the Curve Number are mandatory. The Curve Number (CN) value can be obtained from the hydrologic soil group, land use and moisture conditions of the soil, the last two values being more important.

The SCS-CN method is basically derived on the basis of water balance equation and there are two basic hypotheses (Mishra and Singh 2003). The water balance equation states that:

$$P = I_a + F + Q$$

According to the first hypothesis the ratio of direct runoff to the maximum potential runoff is directly proportion to the ratio of the actual infiltration to the amount of the potential maximum infiltration (retention):

$$\frac{Q}{P - I_a} = \frac{F}{S}$$

According to second hypothesis the amount of initial abstraction can be taken as a fraction of the potential maximum retention.

$$I_a = \lambda S$$

Where

P = total precipitation (mm);

I<sub>a</sub> = initial abstraction (mm);

F = cumulative infiltration excluding I<sub>a</sub> (mm);

Q = direct runoff (mm);

S = potential maximum retention or infiltration;

λ = 0.2

Combining the above equations we get

$$Q = \frac{(P - I_a)^2}{P - I_a + S}$$

The potential maximum soil retention, S, can be calculated using the CN values.

$$S = \frac{25400}{CN} - 254$$

### 2.11.1 Hydrological Soil Groups HSG

Every soil type has a Hydrologic Soil Group (HSG) that indicates an infiltration capacity and a rate of water transmitted through the soil. The four types of HSGs with

brief descriptions are presented in table 2.1. When assigning a HSG to a soil, bare soil surface is considered. The land cover and land use are used in conjunction with these HSG in order to obtain the final value of the Curve Number (CN) parameter.

Table 2.1. Classification of hydrological soil groups by USDA-NRCS 2007

<b>Soil Group</b>	<b>Description</b>	<b>infiltration Rate (mm/hour)</b>	<b>Soil texture</b>
<b>A</b>	Soils have low runoff potential and high infiltration rates. Includes deep sands with very little silt and clay, also deep, rapidly permeable loess.	High Infiltration 8-12	Sand, loamy sand, sandy loamy
<b>B</b>	Moderate infiltration rate and runoff potential. Mostly sandy soils less deep than A, and loess less deep or less aggregated than A, but the group as a whole has above-average infiltration after thorough wetting	4-8	Silt loam, loamy
<b>C</b>	Higher runoff potential and lower infiltration rate. Comprises shallow soils and soils containing considerable clay and colloids, though less than those of group D. The group has below-average infiltration after prostration.	1-4	Sandy loam, loamy
<b>D</b>	Highest runoff potential and very low infiltration rate. Includes mostly clays of high swelling percent, but the group also includes some shallow soils with nearly impermeable sub horizons near the surface.	Lowest infiltration 0-1	Clay loam, silty clay loam, sandy clay, clay

### 2.11.2 CURVE NUMBER CN

The CN is a hydrologic parameter that relies indirectly on the assumptions of extreme runoff events and it is used in determine the potential maximum soil retention (Ponce and Hawkins 1996). The values for the CN for different land use, soil types and soil moisture conditions can be found in the TR-55.

The CN has a value ranges between 0 and 100; a lower numbers indicate low runoff potential while larger numbers indicate higher runoff potential. Lower CN values indicate the lower value of permeability of the soil. Impervious areas and wetlands have higher value of CN.

### 2.11.3 Antecedent moisture condition (AMC)

Curve Numbers are defined on the basis of antecedent moisture condition. AMC represents the amount of moisture in the soil before the precipitation event happens. The term antecedent normally refers to precipitation that has occurred in the previous 5 days. There are three antecedent moisture conditions considering the amount of 5 day precipitation. The range of cumulative precipitation for each AMC is given in the table 2.2.

Table 2.2. Soil AMC for different ranges of cumulative rainfall in dormant and rainy season

AMC	Cumulative 5-days Antecedent Rainfall (mm)	
	Dormant season	Rainfall season
1	<12.7	<35.6
2	12.7-27.9	35.6-53.3
3	>27.9	>53.3

CN are normally defined on the basis of AMC-2 condition but if the soil moisture conditions are for AMC-1 or AMC-2 than the values of AMC are converted using different formulas or tables.

## 2.12 LOSS METHOD FOR HEC-HMS MODEL

HEC-HMS model has different methods for calculating the rainfall loss by the surface e.g. Green and Ampt method, Soil moisture account, SCS curve number etc.

SCS Curve Number (CN) method was used in this study to calculate the initial losses and rainfall excess after the precipitation event. In this method, HSG, LULC and antecedent moisture condition are taken into account with cumulative precipitation in this area. The equation is expressed below:

$$Q = \frac{(P - I_a)^2}{P - I_a + S}$$

Where, Q is the runoff, P is the accumulated rainfall depth at time t; I<sub>a</sub> is the initial abstraction (loss) and S is the potential maximum retention.

### **2.13 TRANSFORM METHOD FOR HEC-HMS MODEL**

The Transform method allows you to specify how to convert excess rainfall to direct runoff .The following dimensionless equation is used for the transformation of surface runoff to the channel:

$$U_p = C \frac{A}{T_p}$$

Where, A is the watershed area and C is the conversion constant (2.08 in SI and 484 in FPS system). The time of peak and duration of the unit excess precipitation is related as:

$$T_p = \frac{\Delta t}{2} t (\text{lag})$$

Where, Δt is the duration of excess precipitation; t (lag) is the basin lag

The lag time is estimated through calibration and this travel time is done by TR-55 method.

### **2.13.1 CN lag Method**

The basin lag time was calculated through CN lag method tool according to the equation below. This equation is based on the curve number method as described in the NRCS National Engineering Handbook, 1972

$$\text{Lag} = \frac{(L^{0.8} * (S + 1)^{0.7})}{1900 * Y^{0.5}}$$

$$S = \frac{1000}{CN} - 100$$

Where: Lag = basin lag time (hours)

L = hydraulic length of the watershed (feet)

Y = basin slope (%)

## **2.14 SENSITIVITY ANALYSIS AND VALIDATION**

Sensitivity analysis is also necessary for accurate flow dynamics, ranking of parameters and their comparative study (Aronica et al., 1998; Bates, 2004; Pappenberger et al., 2008). So it is an obvious criterion for the acceptance of the model to validate the results simulated through it. The observed data is used to compare the simulated result, so the availability of data is a most important criterion here. Validations of the models are done for Tarbela outlet with the observed two years datasets (2000 and 2010). Sensitivity analysis was done for the parameter of Initial Abstraction in the model HEC HMS.

## **2.15 LAND USE LAND COVER CHANGE DETECTION**

Land use illustrates how a piece of land is utilized e.g. as for agriculture or built-up area, while Land cover depicts the materials or resources e.g. vegetation, forest etc.

(Sabins, 1999). Reliable and timely change detection of earth's surface features should be the foundation in order to understand relationships between humans and natural phenomena. It helps in better management and use of available resources. Change Detection is the process in which satellite images of different dates are taken to determine any change in the area for that time span. Change detection procedures should involve data acquired by the same sensor, having the same spatial resolution, viewing geometry, spectral bands, radiometric resolution, and acquired at the same time of day (Lillesand and Kiefer, 2000).

The implementation of the change detection procedure involves several steps. Initially the preprocessing of the raw image is done. The preprocessing includes the image registration and geometrical rectification, radiometric and atmospheric correction and topographic correction if the study area is in mountainous regions. Then a suitable technique is selected to implement the change detection analysis. And finally the accuracy assessment of the image classification as well as change detection is done.

## **2.16 SATELLITE IMAGE CLASSIFICATION**

Classification of satellite images is the process of sorting pixels into a finite number of individual classes, based on their data file values. If a pixel satisfies a certain set of criteria, the pixel is assigned to the class that corresponds to that criteria defined earlier. Classification is the process for sorting and categorizing different landscapes like forests, urban developed land, snow cover areas etc.

The post classification analysis technique involves the independent production and subsequent comparison of spectral classifications for the same area at two different time periods. There are several classification techniques like supervised classification, unsupervised classification, hybrid classification, Object-based classification etc.

Considering the Landsat satellite images; supervised classification and unsupervised classification techniques are normally preferred. In both the methods, low resolution multispectral images are normally classified using traditional pixel based method.

## **2.17 ACCURACY ASSESSMENT OF SATELLITE IMAGE CLASSIFICATION**

Accuracy assessment is most crucial part of examining image classification and thus LULC change detection in order to understand and estimate the changes accurately. It is important to be able to calculate accuracy for individual classification if the resulting data are to be useful in change detection analysis (Owojori and Xie, 2005). Another part that is continuing to get increased attention by research workers is classification accuracy (Lillesand et al, 2000). The post-classification method for LULC change detection has dependency on the accuracy of individual classification results (Foody, 2002). Furthermore the change map of two multi-date classifications of LULC often reveals accuracies similar to the product of multiplying the accuracies of each individual classification. Error in the individual classifications may also be confused with change detection (Khorram, 1999).

### **2.17.1 Error Matrix**

An important method for checking the accuracy of the classification is by comparing the pixels classified with the reference data. Comparison of the datasets is done by generating an error matrix from which different accuracy measures can be calculated. Error matrix compares on category by category basis the relationship between known reference data (ground truth) and corresponding results of automated classification. Matrix is square i.e. number of rows equal to number of categories.

Training pixels that are correctly classified are located along the major diagonal of the error matrix. All non-diagonal elements of Matrix represent error of Omission or Commission. Error of omission refers to those sample points that are omitted in the interpretation results. This corresponds to non-diagonal column elements. Error of commission refers to incorrectly classified samples. This corresponds to non-diagonal row elements. Producer Accuracy-Examined from analysts point of view (column). User Accuracy- Examined from the user's perspective (row).

Overall accuracy is the percentage of correctly classified pixels and is computed as:

$$\text{Overall Accuracy} = \text{OA} = \frac{\Sigma A}{\Sigma B} \times 100$$

Where,  $\Sigma A$  is the sum of pixels assigned to correct classes (diagonal elements), and  $\Sigma B$  is the sum of the total elements of the error matrix.

Similarly, the accuracy for each class also can be computed by dividing the number of correct pixels assigned to the class by the number of pixels that actually belong to that class.

### 2.17.2 Kappa Coefficient

Another measure of statistical classification accuracy can be performed using the kappa ( $\kappa$  hat) index of agreement;

$$k = \frac{N \sum_{i=1}^r x_{ii} - \sum_{i=1}^r (x_{i+} \cdot x_{+i})}{N^2 - \sum_{i=1}^r (x_{i+} \cdot x_{+i})}$$

Where

- $r$  is the number of land cover classes (rows)
- $N$  is the total number of test pixels included in the error matrix
- $\sum x_{ii}$  is total of diagonal elements,
- $x_{i+}$  is the total in row  $i$
- $x_{+i}$  is the total in column  $i$  of the matrix elements

Kappa values are typically between 0 and 1, an indication that the observed classification is that much percent better than the results from chance assignment.

## 2.18 PRECIPITATION MEASUREMENT

Precipitation is any product of condensation of water vapor in the atmosphere falling on the ground in the form of rain, silt or snow. To measure the amount of precipitation falling on ground, rain gauges are used. Rain gauges are considered the most traditional method for measuring rainfall. They have been used historically to provide rainfall amount and rates at a single point in space. The basic idea of most rain gauges is to collect rainwater into a cylindrical vessel of a fixed diameter. Rainfall measurements are usually provided in units of water depth (inches or millimeters).

Point measurements are not the true representation of the overall areal extent of rainfall (Draper et al., 2009). Observational and instrumental errors are major random errors in rain gauge measurements. These (systematic and random errors) may result in up to 30% difference between measured and actual rainfall (WMO, 2006). Moreover, a sparse rain gauge network cannot reflect rainfall variability caused by topography and orography, and will result in erroneous estimates of areal rainfall (Andréassian et al., 2001). The need for more accurate spatially distributed rainfall estimates can be met by satellite based sensors (Huffman et al., 2001).

The number of gauges installed in the Indus Basin is not enough for supporting studies and applications. It is also insufficient for flood warnings, as has been observed during July and August 2010. The Tropical Rainfall Measuring Mission (TRMM) provides regional coverage at higher temporal resolution as compared to other gridded products, but at the cost of a low spatial resolution.

The indirect measurement of precipitation by onboard sensors also has uncertainties (Hong et al., 2006; Hossain et al., 2006). These uncertainties are associated with lack of rainfall detection as well, false detection and bias (Tobin and Bennett, 2010). Both temporal errors ( $\pm 8$  to  $\pm 12\%$  per month) and sampling errors ( $\sim 30\%$ ) can be expected in TRMM rainfall estimates (Franchito et al., 2009). Such errors can result in erroneous applications if applied without calibration (AghaKouchak et al., 2009; Gebremichael et al., 2010). Therefore, TRMM satellite estimates need area specific calibration to reduce such errors.

## **2.19 SATELLITE PRECIPITATION (TRMM) DATA**

Many researchers have used satellite data in hydrological models in un-gauged regions or in regions with meager data (Droogers and Bastiaanssen, 2002; Immerzeel et al., 2008; Winsemius et al., 2008; Wipfler et al., 2011). Calibration and validation of these models need long term data series obtained from dense measurement networks. However, in the basins like Indus, such data lack in quality and the number of gauges is small, thus causing a high level of uncertainty in the model results.

Researchers now days have strong influence on using the remote sensing data for quantifying the precipitation information instead of gauge data due to limitation of small number of gauges and error in the measurements of rain gauges. Satellite data gives continuous temporal and countrywide coverage of precipitation particularly over

unpredictable landscape and un-gauged areas that do not have enough surface based observations. Satellites acquire information about the distribution and amounts of precipitation. Satellite based rainfall estimation methods have been developed for both visible/infrared (VIS/IR) and microwave (MW) instruments. The success of the indirect (VIS/IR) and more directly physical (MW) methods has been very variable depending on the type of precipitating system, the timing of observations and spatial coverage.

Tropical Rainfall Measuring Mission (TRMM) is the joint project between Japan and US launched through the H-II rocket from Tanegashima Space Center of NASDA on November 28, 1997. The mission is first of its kind for measuring the precipitation. TRMM is comprised of 5 sensors namely 1) Precipitation Radar (PR), 2) TRMM Microwave Imager (TMI), 3) Visible and Infrared Scanner (VIRS), 4) Cloud and Earths Radiant Energy System (CERES) and 5) Lightning Imaging Sensor (LIS).

### **2.19.1 Precipitation radar**

The main instrument for estimating precipitation on TRMM satellite is the Precipitation Radar (PR). PR is the most advance among the five instruments of TRMM and is the first instrument of its type which was sent into the space. The main purpose of the PR instrument includes providing a 3-dimensional rainfall structure and to achieve quantitative measurements of the rain rates over both land and ocean.

### **2.19.2 Pakistan rainfall pattern**

In Pakistan rainfall period is highly uneven throughout the year. Generally; the trend of high and low of rainfall can be an indicator of forecasting in planning or flood overcomes the shortage of rainfall associated with drought. The current world climate change has greatly influenced the rainfall pattern either local or global scale.

Remote sensing is being employed to estimate precipitation since late 1970s. Remote sensing estimates of precipitation utilize active and passive sensors. Passive sensors comprise the satellite estimation infrared from cloud properties. Passive sensors are designed to detect naturally occurring energy of solar electromagnetic spectrum reflected by rain droplets or clouds or earth. Typically, to estimate the amount of rainfall is crucial for watching and finding a suitability of observation data which is a weather satellite.

The Daily TRMM 3B42V7 product has been used in order to evaluate the capabilities of the satellite images in accessing rainfall distribution. The purpose of the 3B42 algorithm is to produce adjusted rainfall values of TRMM by merging infrared (IR) precipitation and root mean square (RMS) precipitation error estimates. The final adjusted IR precipitation (mm/hr) and RMS precipitation error estimates are in grid form having a daily temporal resolution and 0.25-degree by 0.25-degree spatial resolution. Spatial coverage extends from 50 degrees south to 50 degrees north latitude.

## **2.20 ADVANTAGES AND DISADVANTAGES OF SATELLITE PRECIPITATION**

Satellite rainfall data have many advantages such as being efficient and cost effective for large areas and having continuous and consistent coverage of large areas. Satellite rainfall observations have emerged in the past decade as a viable data source for a wide range of hydrologic applications at the global scale, including flood modeling and forecasting. Satellite rainfall data validation research has found that the data accuracy can be affected by many factors such as location, climate, period, and rainfall type (Zhou et al., 2008; Sharma et al 2007). In a study on satellite based rainfall estimation, Yilmaz (2005) mentioned that the use of satellite rainfall estimates is more

useful than the use of surface or low altitude precipitation platforms for global hydrology studies.

Although satellite rainfall data offers an effective and economical method for observing rainfall rates and amounts over large areas, the use of satellite rainfall data in global hydrologic studies and modeling remains limited partly because data accuracy remains in question, the datasets are large and cumbersome to use in modeling, and the impact on hydrologic model errors is uncertain.

## **MATERIALS AND METHODS**

### **3.1 DATASETS FOR STUDY**

The remote sensing images like Landsat TM, SRTM DEM and soil map, hydro-meteorological data are used in this study. The detail of the datasets and utilities are discussed below.

#### **3.1.1 Landsat Satellite images**

Landsat imagery was used to produce LULC maps and to carry out change analysis for 10 years period from 2000-2010. The LULC maps were further used in calculating the curve number which is an important input parameter for HEC-HMS model. Landsat satellites images are freely available from the USGS websites. Images were downloaded and extracted for the study area as shown in figure 3.1.

Two Landsat images were used for this research. Both are Landsat TM 5 images which are geometrically corrected level 1A product. One image is of October 2000 and the second image is of November 2010, both the images were 100% cloud free. The thermal band which is low resolution is not used in this research for the image stacking; only the bands 1-5 and 7 are used.

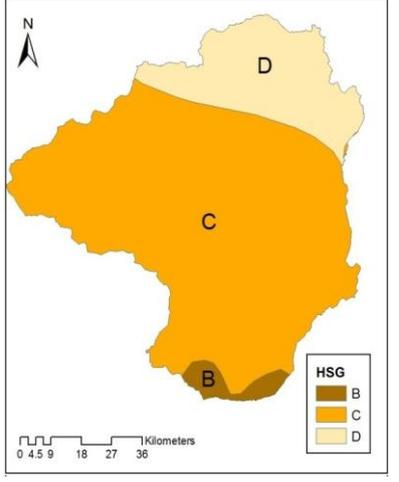
#### **3.1.2 Soil data and HSG map**

The soil characteristics of the study area are very complex due to hilly profile and rapid changes in topography. Different hydrological conditions and slope are also among the main factors of complex soils. The soil map for the study area was acquired from Land and Water Development Division, FAO with name as Digital World Soil Map (DWSM). This data is freely available on the internet. The resolution of the soil

data was 30 arc seconds (approx. 1 km). Extraction of the data for the study area resulted in 3 soil groups which have the following characteristic.

Table 3.1. Dominant soil types and Hydrological Soil Group in the study area obtained from World Digital Soil Map (WDSM).

Soil Texture	Dominant Soil Series	Percentage of Dominant Soil in the Mapping Unit	HSG
Silt loam, loamy	Abottabad, Badwan, Buner	70%	<b>B</b>
Sandy loam, loamy	Gulibagh, Mansehra	50%	<b>C</b>
Clay loam, silty clay loam, sandy clay, clay	Baragali, Mingora	34%	<b>D</b>



### 3.1.3 Topographic data

Satellite based topographic data is a major development in hydrological modeling. It contains elevation data for regularly spaced grid intervals over the surface of the earth. The interval in the grid is referred to as a pixel. The Digital elevation model pixel size has an important role in hydrological modeling. Low resolution DEM always gives the average and less information about the small features and land surface areas of complex relief.

The Shuttle Radar Topographic Mission (SRTM) by NASA provides digital elevation data (DEMs) for more than 80% of the globe. This data is currently available free of cost by USGS and can be downloaded from the USGS ftp site. The SRTM data for the study area is available at 3 arc second resolution (approx. 90m).

### 3.1.4 Hydro-Meteorological data

Daily discharge data for the years 2000 and 2010 was acquired from the Federal Flood Commission (FFC), Pakistan. The data was analyzed and errors were rectified.

The data was plotted in the form of hydrograph and the outlying values as well as missing values were sorted out. The data was used for model calibration and validation purpose.

### **3.1.5 Remote Sensing (TRMM) Precipitation Data**

Satellite (TRMM) based daily precipitation estimates of 3B42V7 were downloaded from the internet. The web link for the data is [ftp://disc3.nascom.nasa.gov/data/s4pa/TRMM\\_L3/TRMM\\_3B42\\_daily](ftp://disc3.nascom.nasa.gov/data/s4pa/TRMM_L3/TRMM_3B42_daily). Precipitation data is the most important input parameter for the HEC-HMS model. The TRMM precipitation estimates are available with a resolution of a near global 0.25° x0.25° grid over the latitude band 50° N-S. TRMM daily precipitation data was downloaded for two years (2000 and 2010) in Binary (.BIN) format. The preprocessing of TRMM data after download is described below.

## **3.2 DATA PROCESSING**

Data processing involves the processing of satellite imagery, soil data extraction, producing curve number raster for the model, HEC-GeoHMS model processing and setting of input parameters and processing for discharge calculation through HEC-HMS model.

### **3.2.1 Landsat image processing**

Considering the topography and extent of the study area, unsupervised classification did not give satisfactory results because of huge number of the mix classes. So a much more successful approach is the supervised classification using maximum likelihood classifier technique.

These applications were carried out using ERDAS imagine and Arc Map software. After the initial steps of stacking the layers and sub-setting of the image, the image enhancement and corrections were made. Training sites were created for 5 major categories which are:

- Water
- Soil
- Forest
- Grasslands
- Built-up area

A total of 75 training sites were selected for each image. A high resolution Google image was used to perform the ground verifications. Also for validating the results, Google Earth was used. Historical images tool was used for 2000 image. This procedure was important to carry out because the ground verifications physically were not possible due to the security issues in the study area.

The accuracy assessment of the images was done using high resolution Google imagery. Error matrix was generated and user accuracy as well as producer accuracy and the overall accuracy was calculated.

### **3.2.2 Generation of Curve Numbers**

Importance of curve number was illustrated in the introduction chapter. CN is used for loss model in HEC-HMS model. Primarily it is prepared from the combination of LULC and soil map with the help of literature (US-SCS, 1986). The soil property which is used in generation of curve number is Hydrological Soil Group (HSG). Then it is

optimized in HEC-HMS manual trial and error method. The following steps are done to get a Curve Number grid for the area of interest from LULC and HSG maps:

- Both LULC map and soil maps were converted to polygons.
- Table or vector operation (Union) to get polygons of unique combination of both the maps in Arc-GIS.
- CN values for each unique combination of polygons were assigned by query operation in Arc-GIS and grid map was created.
- Raster map of CN was generated as shown in the fig
- Average CN value determination for each sub-basin.

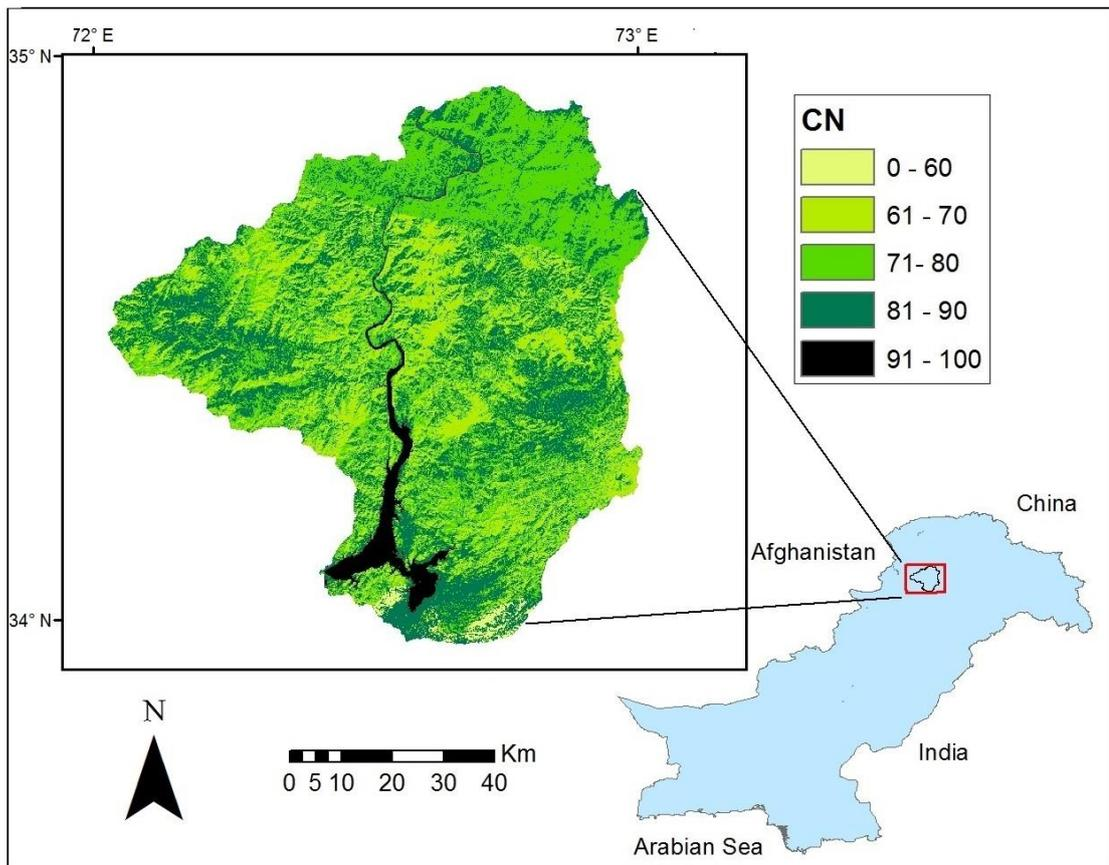


Figure 3.1. Curve Number Raster generated from LULC and Soil data. The dark shades represent higher value of CN and thus higher runoff potential areas while the brighter colors represents lower runoff potential areas.

### 3.2.3 Processing of Precipitation Data

TRMM daily precipitation data was downloaded in Binary (.BIN) format. Each daily precipitation data file was converted from binary format into ASCII format using matlab code given at

[ftp://disc2.nascom.nasa.gov/data/TRMM/Gridded/Derived\\_Products/3B42\\_V7/Daily/readme](ftp://disc2.nascom.nasa.gov/data/TRMM/Gridded/Derived_Products/3B42_V7/Daily/readme) as shown below:

```
A sample program in Matlab
% This program is to read a TRMM 3B42 daily binary file

fid = fopen('3B42_daily.2003.01.01.7.bin', 'r');
a = fread(fid, 'float','b');
fclose(fid)

data = a';

count = 1;
for i_lat = 1:400
    for j_lon = 1:1440
        lat = -49.875 + 0.25*(i_lat - 1)
        if j_lon <= 720
            lon = 0.125 + 0.25*(j_lon - 1)
        else
            lon = 0.125 + 0.25*(j_lon - 1) - 360.0
        end
        daily_rain_total = data(count)
        count = count + 1;
    end
end.
```

ASCII files obtained after running the code were then converted into Raster format using ASCII to RASTER conversion tool in ARCGIS. The conversion was conducted on the data for 2000 and 2010 years.

### 3.3 ANALYTICAL FRAMEWORK

The analytical framework represents the overall methodology followed during the research work. It includes the data collection, data pre-processing, model processing through

calibration and validations and finally the analysis of the results obtained. The flow chart is given in the figure 3.3.

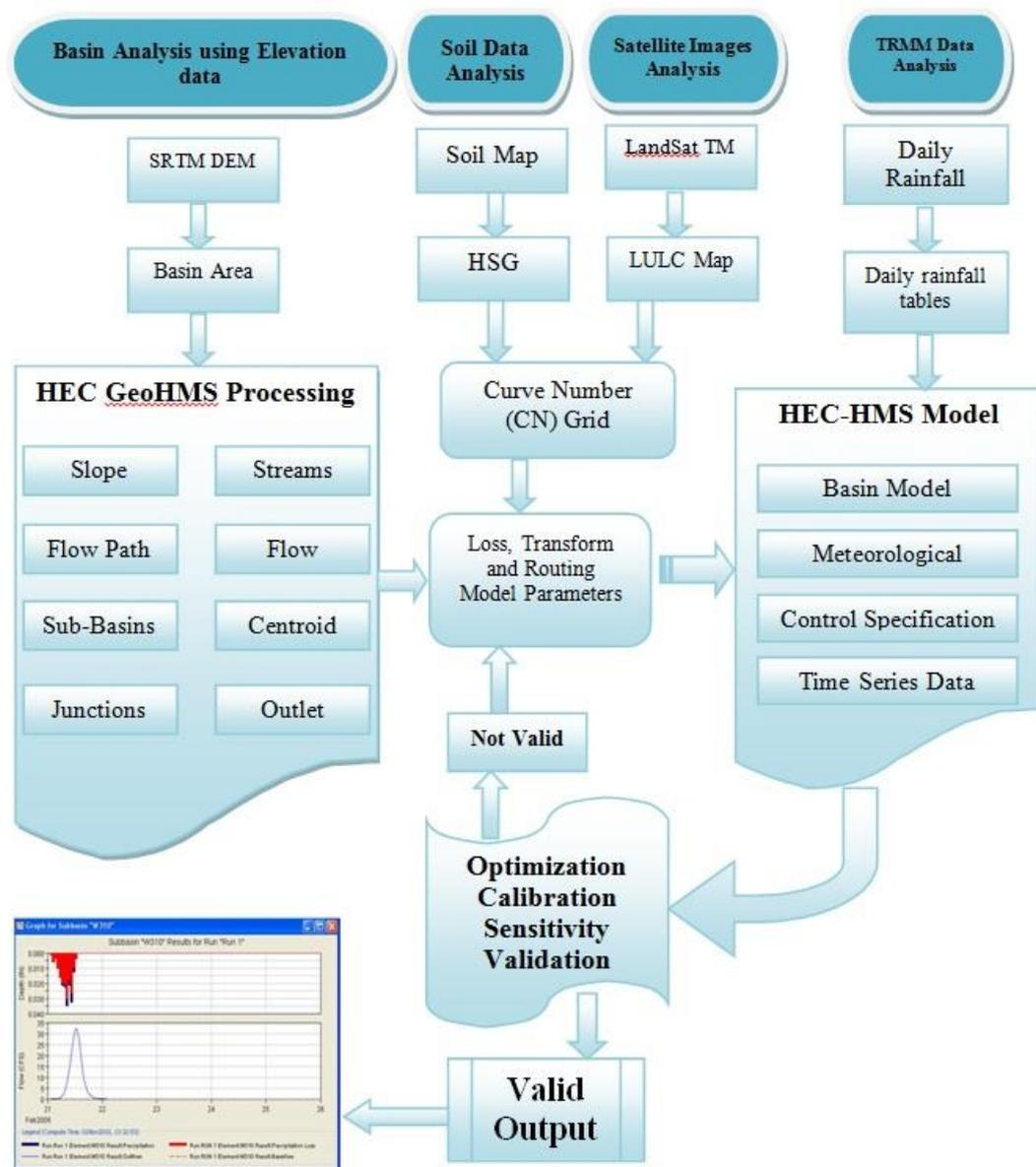


Figure 3.2. Overall methodology for carrying out the research. It has four major parts; 1) DEM processing, which was done in HEC-GeoHMS extension of ArcGIS; 2) Soil map was processed to extract Hydrological Soil Groups for the study area; 3) precipitation data was downloaded and converted to input in the model HEC-HMS; 4) satellite images were classified to produce LULC maps. All the data was given in the model and after calibration and optimization, valid results were produced.

## **3.4 HEC-GEO HMS PROCESSING**

### **3.4.1 DEM Hydrological Processing**

Before going to the HEC-HMS part, the terrain processing is needed. HEC GeoHMS extension in ArcGIS was used for DEM hydrological processing, and then it is used for further basin processing and defining the parameters necessary for generating a HEC-HMS model. The SRTM 90m grid format is input file type as a DEM. The Several hydrological maps are generated step by step. Initially 53 sub-watersheds are primarily formed few of them were merged and the final number of sub-watersheds were 48. The following physical parameters are generated from DEM processing:

- Fill Sink
- Flow Direction
- Flow Accumulation
- Stream Definition
- Watershed Delineation
- Watershed Polygon Processing
- Stream segment Processing
- Watershed Aggregation

### **3.4.2 Generating a Project**

After the completion of the DEM hydrological processing, basic input data was completed. A new project was generated that will be used to develop the necessary input parameters information to create an HEC-HMS project. The project was setup after specifying a control point which is defined as an outlet point of the watershed.

After defining the downstream outlet, HEC-GeoHMS will extract data from the datasets created using the terrain preprocessing tools for the drainage area upstream of the outlet.

### **3.4.3 Threshold Value for Project**

The number of sub-watersheds depends upon the threshold area value. The threshold is used to classify all flow accumulation cells with a flow accumulation greater than the user-defined threshold as cells belonging to the stream network. A smaller threshold will result in more streams and sub-basins. Here 53 sub-basins are created automatically with a threshold value of 67 Km<sup>2</sup>. Then few sub-watersheds are merged and finally 48 sub-basins are created to get outflow hydrographs from HEC-HMS

### **3.4.4 Basin Processing**

Small basins are merged intentionally to achieve the hydrographs of only predetermined particular locations with the help of Topographical sheets. Basin and river slopes were also calculated and the values for the respective terms were stored in their attribute tables.

### **3.4.5 Longest Flow Path Calculation**

Longest flow path in the whole basin was calculated or for all sub-basins. The longest flow path value was calculated for travelling time calculation to be done in the HEC-HMS.

### **3.4.6 Basin Centroid and Centroidal Flow Path**

Basin centroid was calculated. Depending upon the purpose and characteristics of the basin (mainly shape), different methods are used for better result. These methods

include; center of gravity, longest flow path and 50 percent area. For this study the flow path method was used i.e. the centroid as the centre of longest flow path.

#### **3.4.7 Sub-Basin Parameters through Raster**

The next step is to assign the Curve Number CN to the project. This is done through the tool Sub-basin parameters through raster. In this tool the raster layer of CN is given as an initial loss grid. In this tool only those parameters can be added as input which could be estimated using geospatial data. The remaining parameters can be entered manually in HEC-HMS model and then are determined by calibrating the HEC-HMS model to historic rainfall runoff events.

#### **3.4.8 CN lag Method**

The basin lag time was calculated through CN lag method tool according to the equation which is based on the curve number method as described in chapter 1. Lag time calculated was in minutes.

#### **3.4.9 Generation of Files for HEC-HMS**

To run the model and parameters setting in HEC-HMS model, 3 model files are generated namely 1) Basin model file 2) Meteorological model file and 3) gauge file. The basin model captures the hydrologic elements, their connectivity, and related geographic information. The gauge file is generated using specified hyetograph method which allows the user to enter total storm depth value for each sub-basin in HEC-HMS model.

### 3.5 HEC-HMS MODEL SETUP

After defining the complex physical processes using ArcGIS tool of HEC-GeoHMS, the generated model was processed further in HEC-HMS model. HEC-HMS has four main model components:

**Basin model:** contains information relevant to the physical attributes of the model, such as basin areas, river reach connectivity, or reservoir data.

**Meteorological model:** contains the rainfall, evapotranspiration data.

**Control specifications:** contains information pertinent to the timing of the model such as when a storm occurred and what type of time interval is to be used in the model, etc.

**Input data:** stores parameters and boundary conditions for basin and meteorological models (HEC, 2006).

#### 3.5.1 Basin Model

The Basin model consists of the hydrologic element and how they are connected to each other i.e. it represents how water moves through the drainage system. The basin model actually converts the atmospheric conditions of precipitation, evapotranspiration etc. into stream flow at different locations in the watershed (HEC, 2006b). Basin model background file was created in HECGeoHMS, which is an ArcMap extension developed by the U.S. Army Corps of Engineers (USACE) after delineating the sub-catchments from the DEM. The hydrological components of basin model are spatially set through the background maps file.

The CN used is an optimized value through trial and error method from primarily used values. This SCS Unit Hydrograph method is used here for loss model because it's a simple event based lumped and widely used stable model. It is also

depended on the availability of dataset and moreover remote sensing and GIS technique are also applicable in this method.

Table 3.2. 48 sub-basins were generated by HEC-GeoHMS . Sub-basin wise elements details of some of those sub-basins are given in the table. Unit hydrograph was selected as Transform method, SCS-CN as loss method and CNlag as the lag method to generate these elements.

Sub-basin	Area (sq.km.)	Basin Lag (Hr)	Basin CN
W540	389.48	2.88	82.30
W550	125.05	1.18	81.04
W590	122.21	1.50	78.81
W630	256.04	2.08	80.12
W690	338.01	3.08	77.08
W730	162.77	1.74	76.89
W830	77.26	1.73	75.13
W910	41.43	1.37	83.55
W920	434.79	3.74	79.70

### 3.5.2 Meteorological Model

Through the meteorological model the precipitation data is distributed spatially and temporally over the watershed for computations. Time series of daily precipitation is the input in this model. Daily precipitation data from 15 July to 15 September was used as input. The units for rainfall data is millimeter (mm).

### 3.5.3 Control Specification

Control specifications are one of the main components of a project, and principally used to control simulation runs. They control when a simulation starts and stops, and what time interval is used in the simulation. A simulation run was created by combining a basin model, meteorological model, and control specifications.

The data input to HEC-HMS is possible through two ways. The first and simplest method is manual data input. Here the time series data is copied from Excel or any compatible format and pasted in HEC-HMS time series table for any time series

data (either precipitation or discharge). The second and relatively complex is saving the data in HEC-DSS and retrieving from it during analysis. For this study, manual data input method is used because this method is simple one.

The start date of the simulation was 15 July and ending date was 15 September 2000. The interval set for the model was 1 day. So the total numbers of days for the simulation were 63 days in the monsoonal period.

### **3.6 MODEL CALIBRATION AND VALIDATION**

Model calibration involves modification of sensitive parameters, within an acceptable range, in an attempt to match model output to measured data based on a predefined objective function. During calibration, parameters estimated from model are compared with referenced observations. Generally, a hydrological model needs some form of calibration before it can be used in an area other than where it was originally developed. In automatic models the calibration is done by the model itself to reach value which is best fit. But the manual calibration of model requires knowledge about the basin as well as the hydro-processes (CFCAS, 2004).

During the calibration phase the user identifies the processes which govern the overall system of the river basin. For example if the runoff volume is less than the rainfall volume it shows that the water is lost through infiltration and if the volume is greater than the rainfall volume, it indicates that base flow is adding to the total flow.

After calibration the model is verified by simulating it on any other data keeping the model parameters to the same values as those in the calibration phase. The verification model simulation depicts the accuracy of the model and its capability to various scenarios of rainfall-runoff modeling.

## 3.7 STATISTICAL TEST

Different statistical tests are applied in hydrology to check the accuracy of the results obtained through models in the process of calibration and validation. A brief description of three statistical tests applied in this research to check the accuracy of the results is given below.

### 3.7.1 Correlation Coefficient

Correlation Coefficient relates the simulated and observed data linearly and represents the direction and strength of the data. The most common correlation coefficient is the Pearson correlation coefficient which is the linear correlation between two variables or datasets. The range of PCC is between  $-1$  and  $1$ , where positive  $1$  represents complete positive correlation,  $0$  represents no correlation and negative  $1$  represents total negative correlation (Santhi et al., 2001). If we have a series with  $n$  ground observations and  $n$  estimated values, then the PCC can be used to estimate the correlation between model and observations.

$$\text{Correlation Coefficient} = \frac{\sum_{i=1}^n (P_G - \bar{P}_G)(P_S - \bar{P}_S)}{\sqrt{\sum_{i=1}^n (P_G - \bar{P}_G)^2} \cdot \sqrt{\sum_{i=1}^n (P_S - \bar{P}_S)^2}}$$

Where

$P_G$  = Ground Based Precipitation

$\bar{P}_G$  = Average Ground Based Precipitation

$P_S$  = Satellite Based Precipitation

$\bar{P}_S$  = Average Satellite Based Precipitation

$n$  = Time Period

### 3.7.2 The Relative Bias (BIAS)

It describes the systematic bias of simulated and ground observed data for a model simulation. Negative bias values shows the underestimation of simulated data with respect to the observed data while the positive values shows the over estimation of values.

$$\text{Relative Bias} = \frac{\sum_{i=1}^n (P_S - P_G)}{\sum_{i=1}^n (P_G)}$$

### 3.7.3 Nash–Sutcliffe Coefficient of Efficiency

The Nash–Sutcliffe model efficiency coefficient is used to assess the predictive power of hydrological models.

$$\text{NSCE} = 1 - \frac{\sum_{i=1}^n (R_{obs,i} - R_{sim,i})^2}{\sum_{i=1}^n (R_{obs,i} - \bar{R}_{obs})^2}$$

Where

$R_{obs}$  = Discharge observed

$R_{sim}$  = Discharge Simulated

$\bar{R}_{obs}$  = Average observed discharge

Nash–Sutcliffe efficiencies can range from  $-\infty$  to 1. The value of positive 1 ( $E = 1$ ) represents a complete matching of simulated and observed values of discharge. The value 0 ( $E = 0$ ) shows that the simulated values from model are as accurate as the mean of the observed data, whereas a value of less than zero ( $E < 0$ ) occurs when the observed mean is a better predictor than the simulations from model.

Nash-Sutcliffe efficiency coefficient normally overestimates the model simulated values during peak flows while underestimates the model simulated values in low flow conditions. This is because of the fact that squared values of difference between observed and simulated discharge are used which overestimates the larger values and underestimates the smaller values (Legates and McCabe, 1999).

## **RESULTS AND DISCUSSIONS**

The current research study focuses on finding the land use land cover change in the Arbela watershed area for 10 year period. The results for those finding will be helpful in determining the impact of changes in LULC on the hydrological response on the area. The resulting maps of LULC were used in hydro-modeling the discharge for the watershed using HEC-HMS model.

### **4.1 LULC CHANGE ANALYSIS**

Supervised image classification was used to classify the Landsat satellite images of 2000 and 2010 using maximum likelihood classifier. Supervised classification uses suitable methods to label specific pixels in an image as representative ground cover classes. Five classes were made namely; Water, Soil, Forest, Grass and Built-up. Mixed pixel classes and some shadow in the images were sorted out using high resolution imagery and the areas with some anomalies were classified into the respective classes. The final LULC maps for the years 2000 and 2010 are shown in figure 4.1.

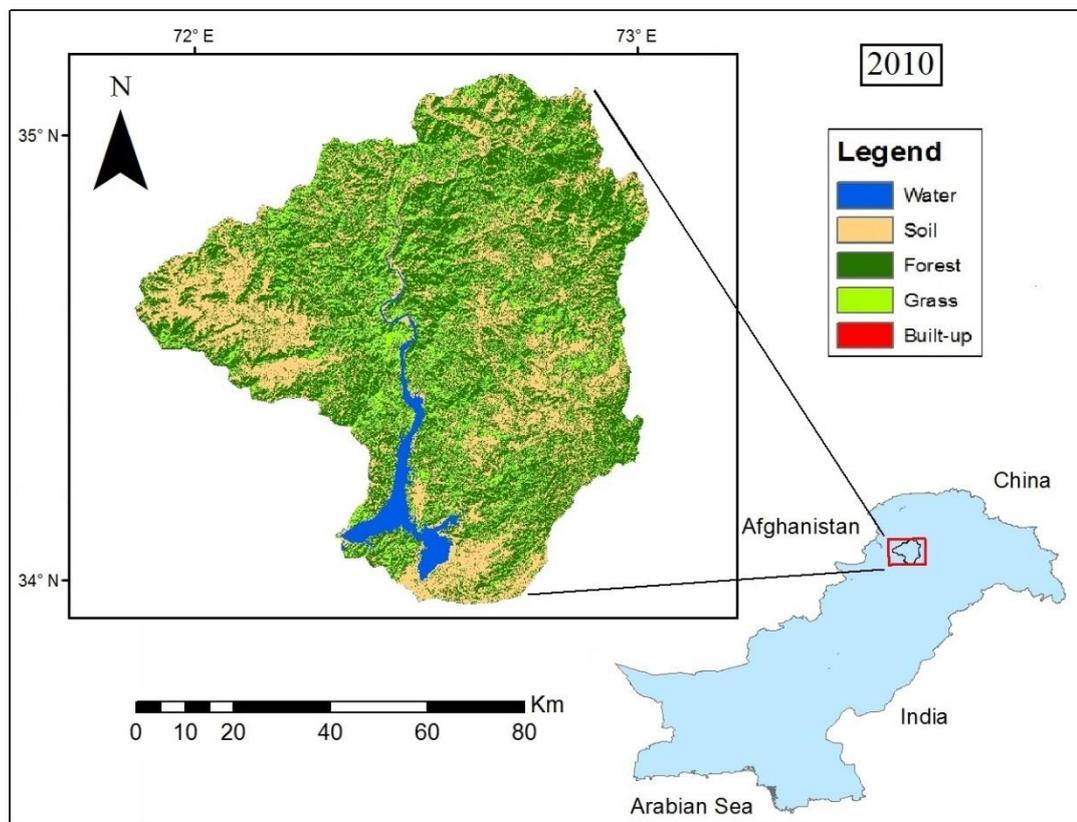
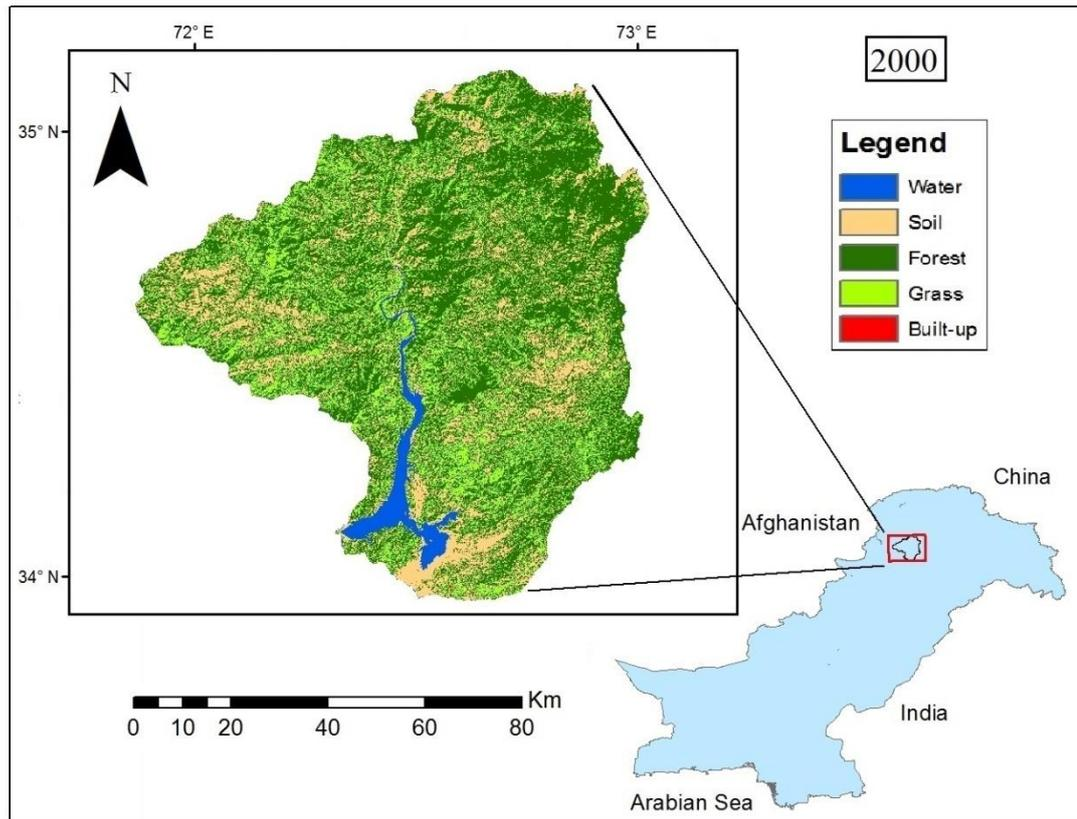


Figure 4.1. LULC map of 2000 and 2010 produced after supervised image classification of the Landsat satellite images. The LULC classes include soil, forest water, grass and built-up area.

## **4.2 ACCURACY ASSESSMENT FOR 2010 LANDSAT IMAGE CLASSIFICATION**

The error matrix was made through high resolution Google imagery. Total 98 points were taken on the Google image for different land covers and then they were validated by overlaying them on the classified image of 2010. Error matrix for each land cover class is shown in the table 4.1. The overall accuracy was calculated as 71.4%. The kappa coefficient is the measure of statistical classification accuracy. The kappa coefficient for the 2010 image was calculated as 0.623

## **4.3 LULC CHANGE**

The result of supervised image classification shows a change in land use land cover in the area of main classes. Three important classes which dominate in setting the trend of runoff in the study area are grass, forest cover and soil. Soil cover area showed increasing trend while grass and forest area showed decreasing trend. Although the built-up has increased more than two times in the ten year period, but still this area has very little impact on the overall study area. Built-up area is found to be less than 1% of the total area in 2000 and 2010 images. The details of the LULC classes and their change is given in the table 4.2. The bar graph shown in the figure 4.2 gives a good illustration of the results for 2000 and 2010 LULC change.

Table 4.1. Error matrix generated for accuracy assessment. The diagonal elements show the accurately classified pixel values. Table also show the user accuracy and producer accuracy

	<b>Water</b>	<b>Soil</b>	<b>Forest</b>	<b>Grass</b>	<b>Built-up</b>	<b>Row Total</b>	<b>User accuracy</b>
<b>Water</b>	8	1	0	0	1	10	80.00
<b>Soil</b>	1	23	0	3	2	29	79.31
<b>Forest</b>	0	0	14	6	0	20	70.00
<b>Grass</b>	0	6	2	14	0	22	63.64
<b>Built-up</b>	0	6	0	0	11	17	62.50
<b>Column Total</b>	9	36	16	23	14	98	
<b>Producer accuracy</b>	88.89	63.89	87.50	60.87	78.57		

Table 4.2. LULC types and corresponding area for the year 2000 and 2010. Percentage increase or decrease in area is also calculated.

Land Cover Type	Area in year 2000 (sq.km)	percentage of total area 2000	Area in year 2010 (sq.km)	Percentage of total area 2010	Percentage increase/decrease
Water	204.77	3.01%	225.73	3.32%	Increase 10%
Soil	2343.55	34.40%	3075.56	45.20%	Increase 31%
Forest	2280.31	33.47%	1892.56	27.81%	Decrease 17%
Grass	1962.29	28.81%	1563.76	22.98%	Decrease 20%
Built-up	21.55	0.32%	48.30	0.71%	Increase 124%

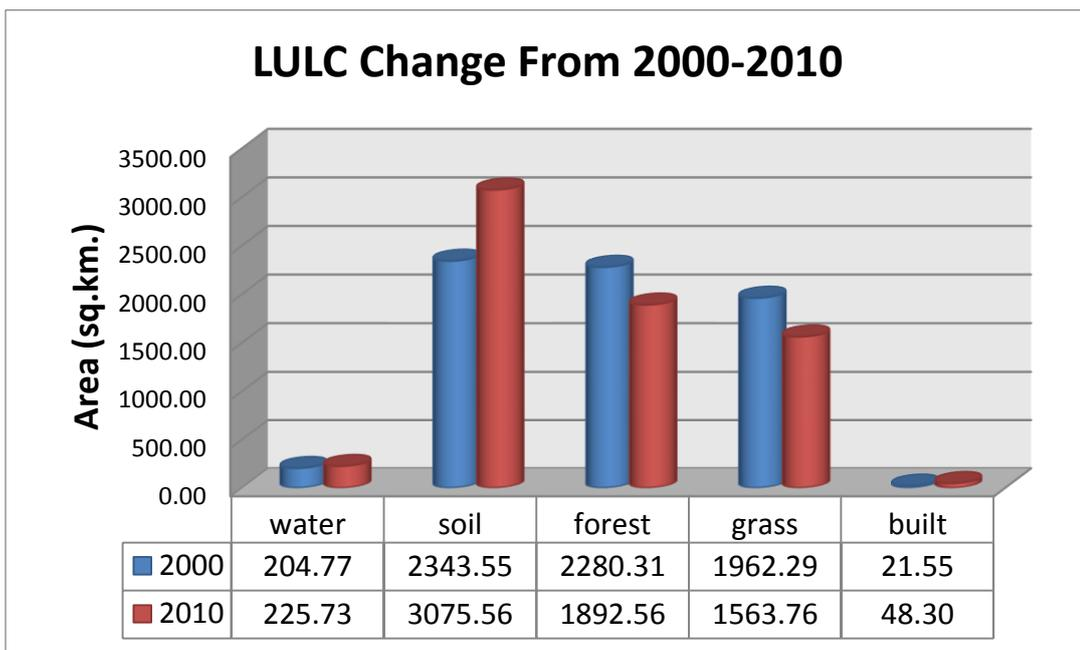


Figure 4.2. Bar graph showing comparison of change in each LULC class from 2000 to 2010

#### **4.4 CALIBRATION AND VALIDATION OF HEC-HMS MODEL**

HEC HMS model was calibrated using the 2000 datasets and parameters setting. The discharge data from FFC was used in the calibration. The parameters including initial abstraction and curve number were tuned to best possible match for the observed ground discharge data. The 2010 dataset was then used for validation purpose keeping the parameters values same as that of 2000.

#### **4.5 HEC-HMS MODEL RESULTS**

In this study, discharge analysis for monsoonal period of years 2000, and 2010 was done. Satellite rainfall data (TRMM) for the months of July, August and September was used to simulate the discharge in the HEC-HMS model. The time period was selected because the flood event or high discharge normally occurs in this time period. The simulated result is taken into consideration for Tarbela outlet. The model was run with one day time interval and the analysis is based on this output dataset. Per day simulated (average) discharge is used to compare with daily average observed discharge. Some selected values of the simulated and observed discharge for one day period is shown in table 4.3. The optimized value is used for simulated hydrographs generation for the years 2000 and 2010 as shown in figure 4.4 and figure 4.5 respectively.

Table 4.3. Observed and model simulated discharge for random days of 2000 and 2010

Date	2000			2010		
	Precipitation	Observed	Simulated	Precipitation	Observed	Simulated
19 Jul	2.3	5390	4732.20	41.71	8495.2	9539.62
22 Jul	12.4	4793.6	5238.00	12.66	9780.4	9747.57
26 Jul	0.0	6843.2	7034.30	24.20	6199.2	6626.25
27 Jul	1.5	6988.8	6912.90	11.34	6686.4	7570.85
28 Jul	4.7	6834.8	6985.80	38.69	7837.2	9523.4
29 Jul	16.0	6955.2	7466.40	120.97	12852	15745.05
31 Jul	74.5	8008	9769.50	0.13	15307.6	12152.07
6 Aug	29.4	5616.8	5485.50	23.51	10480.4	10772.59
9 Aug	18.4	5269.6	5258.70	0.75	14761.6	15751.64
10 Aug	1.6	5667.2	5501.70	19.77	15598.8	14606.9
19 Aug	0.1	4858	4923.90	14.88	9730	9333.95
23 Aug	2.4	3925.6	3786.30	28.49	8450.4	8992.84
24 Aug	0.1	3852.8	3458.70	19.37	7996.8	8438.75
31 Aug	13.4	4874.8	5106.60	0.26	4762.8	4152.71
4 Sep	10.5	4715.2	4454.10	3.00	5933.2	5368.44
6 Sep	20.2	4603.2	4533.30	0.18	5577.6	4939.14

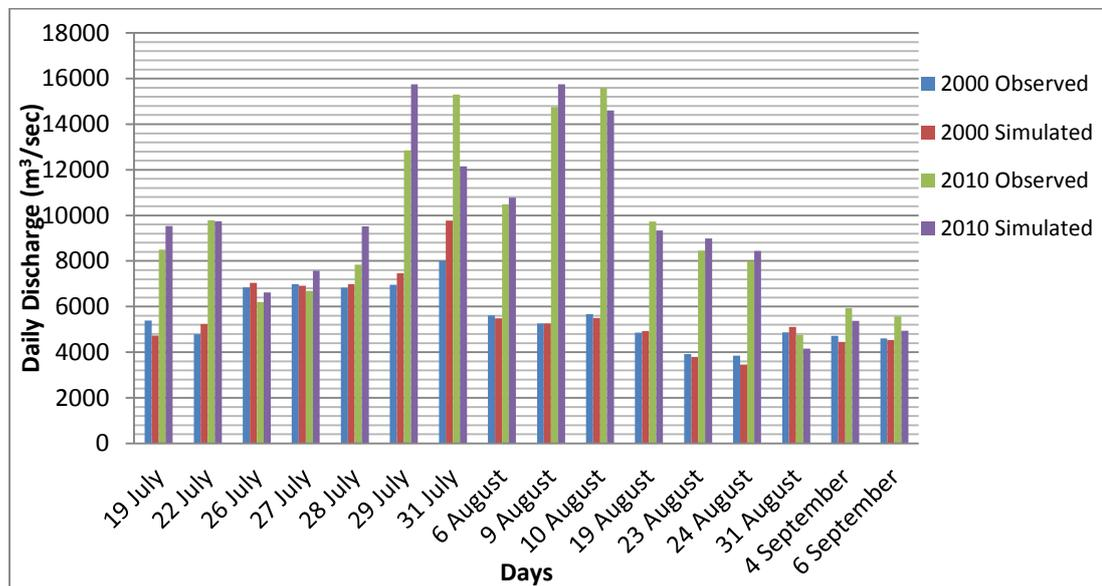


Figure 4.3. Bar graph showing comparison of observed and simulated discharge for rainfall event days selected for year 2000 and 2010 (15 July to 15 September)

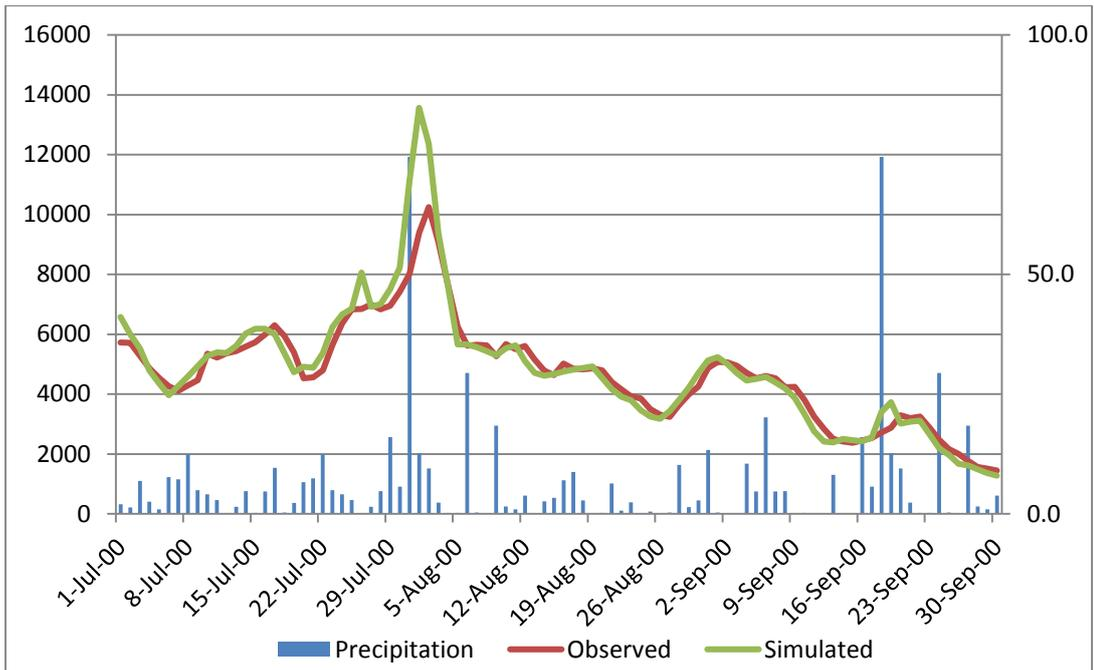


Figure 4.4. Comparison of simulated discharge for 2000 generated by the model after calibration, plotted versus the observed discharge values at Tarbela outlet

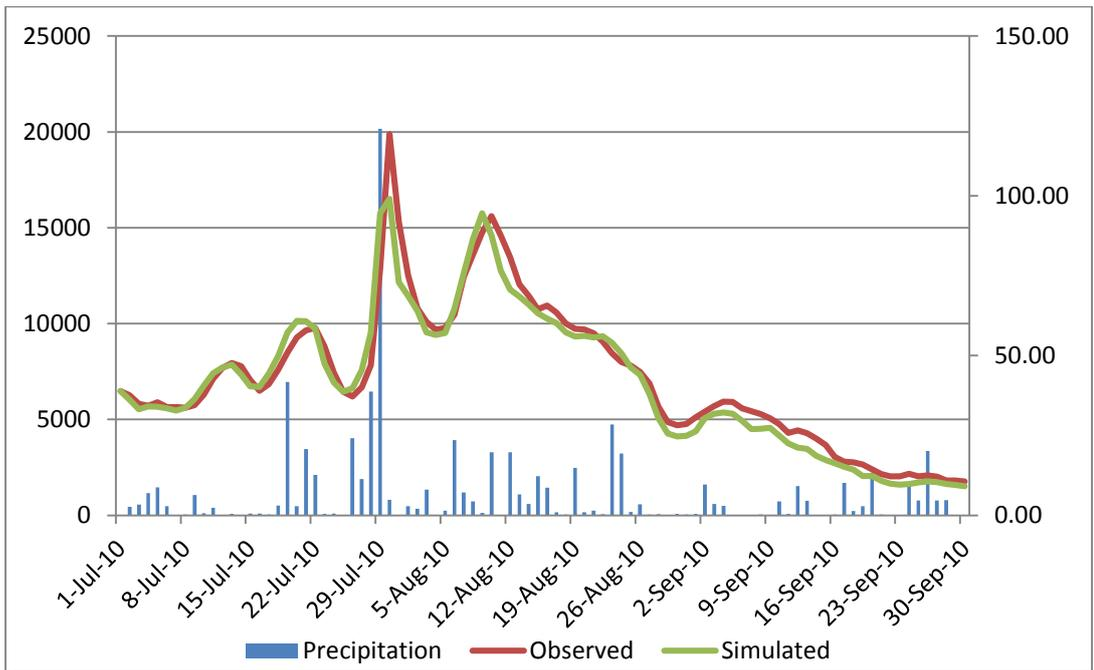


Figure 4.5. Comparison of simulated discharge for 2010 generated by the model after calibration, plotted versus the observed discharge values at Tarbela outlet

#### 4.5.1 Statistical Analysis of Results

Different statistical methods are used to evaluate the accuracy for the results produced by the HEC-HMS model. The theory of those methods is already discussed in chapter 3. The results of the tests are given in table 4.4 and figure 4.6.

Table 4.4. Statistical analysis results

Statistical method	2000	2010
Correlation coefficient	0.96	0.97
Nash-Sutcliffe Efficiency	0.87	0.91
Relative Bias	-9%	-14%

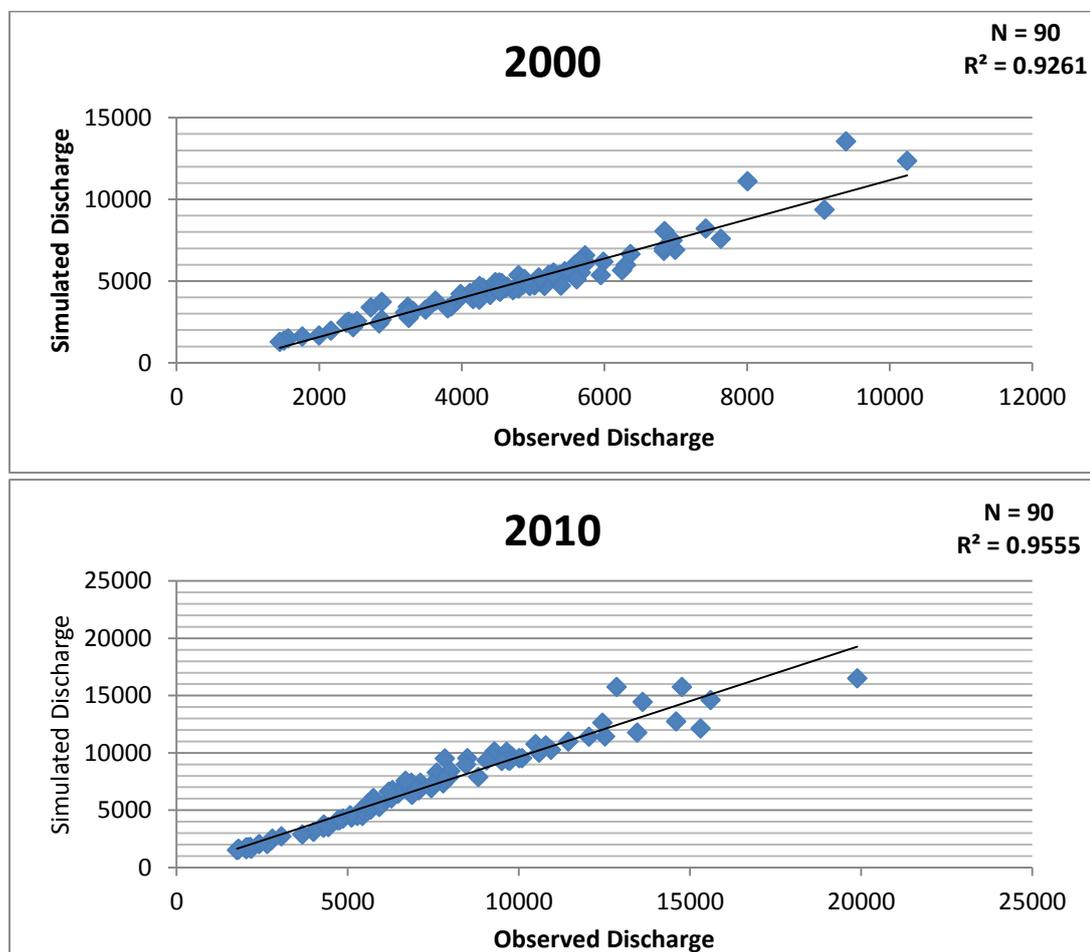


Figure 4.6. Scatter plot for 3 months (July-September) with regression line between observed and simulated discharge for 2000 and 2010

## 4.6 SENSITIVITY ANALYSIS OF HEC-HMS

During the calibration process for HEC-HMS, two parameters were found more sensitive. These are the Curve Number (CN) and Initial Abstraction for sub-basins. Three values for all of the parameters are used to get how they are sensitive and which is more sensitive and which is most sensitive for Tarbela watershed. It is found that the Curve Number comes out as the most sensitive parameter to change the discharge value followed by Initial Abstraction. The sensitivity index for the parameters was also calculated using the following equation

$$S_i = \frac{|R_I - R_D|}{R_n}$$

Where,      Si =    Sensitivity Index  
              RI =    Parameter increased  
              RD =    Parameter decreased  
              Rn =    Parameter value

The result of the sensitivity index is shown the figure 4.7.

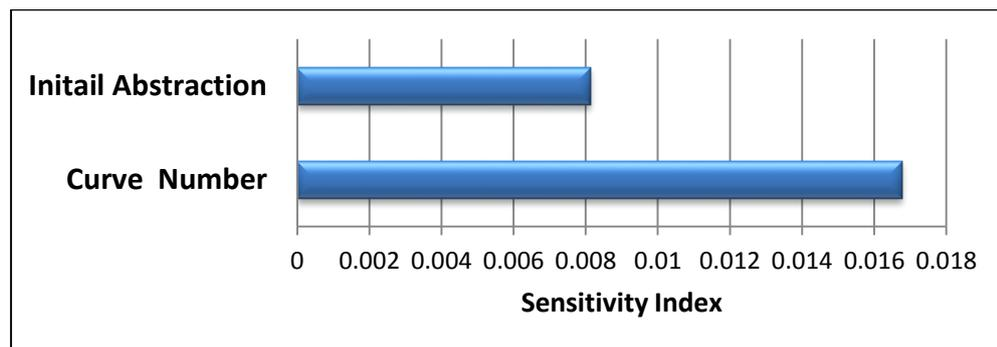


Figure 4.7. Sensitivity index for the parameters showing the more sensitive parameter of CN and less sensitive parameter of initial abstraction.

#### **4.6.1 Sensitivity Analysis for Curve Number**

Sensitivity analysis for the curve number using three scenarios was done. The three scenarios were created considering the antecedent moisture condition (AMC). The three AMC conditions depends on the amount of cumulative precipitation occurred in the 5 previous days from the day of simulation. AMC-1 refers to less than 33 mm cumulative precipitation, AMC-2 refers to cumulative precipitation of 33mm to 52 mm while AMC-3 refers to cumulative precipitation of more than 52 mm. The best results were found when the CN2 values were used for AMC condition 2 as shown in the figure 4.8.

#### **4.6.2 Sensitivity Analysis for Initial Abstraction**

Initial abstraction is important parameter in determining the loss of precipitation by soil. Three scenarios were created to analyze the sensitivity of the model simulation to initial abstraction. Initial abstraction value which gives the better result was 8 mm.

Table 4.5. Sensitivity analysis values for curve number parameter. The corresponding discharge values for each CN are given along with the observed discharge at Tarbela gauge.

Date	CN1	CN2	CN3	Observed
22-Jul-00	5241.3	5246	5252.8	5238
29-Jul-00	7476.8	7489.3	7509.7	7466.4
31-Jul-00	10251.3	10514.9	10784.3	9769.5
1-Aug-00	12429.9	12760.9	13100.4	11872.8
2-Aug-00	12284	12304.1	12324.8	12263.4
6-Aug-00	5589.7	5674.1	5790.1	5485.5
9-Aug-00	5299.5	5336	5391	5258.7
28-Aug-00	4165.8	4166.6	4167.1	4164.3
31-Aug-00	5111.7	5118.4	5129	5106.6
4-Sep-00	4455.7	4458.8	4462.6	4454.1
6-Sep-00	4555.6	4579	4618.2	4533.3
7-Sep-00	4371.1	4399	4444.3	4347.9
9-Sep-00	3866.2	3871.4	3880.1	3861
10-Sep-00	3334.7	3342.6	3354.3	3329.1

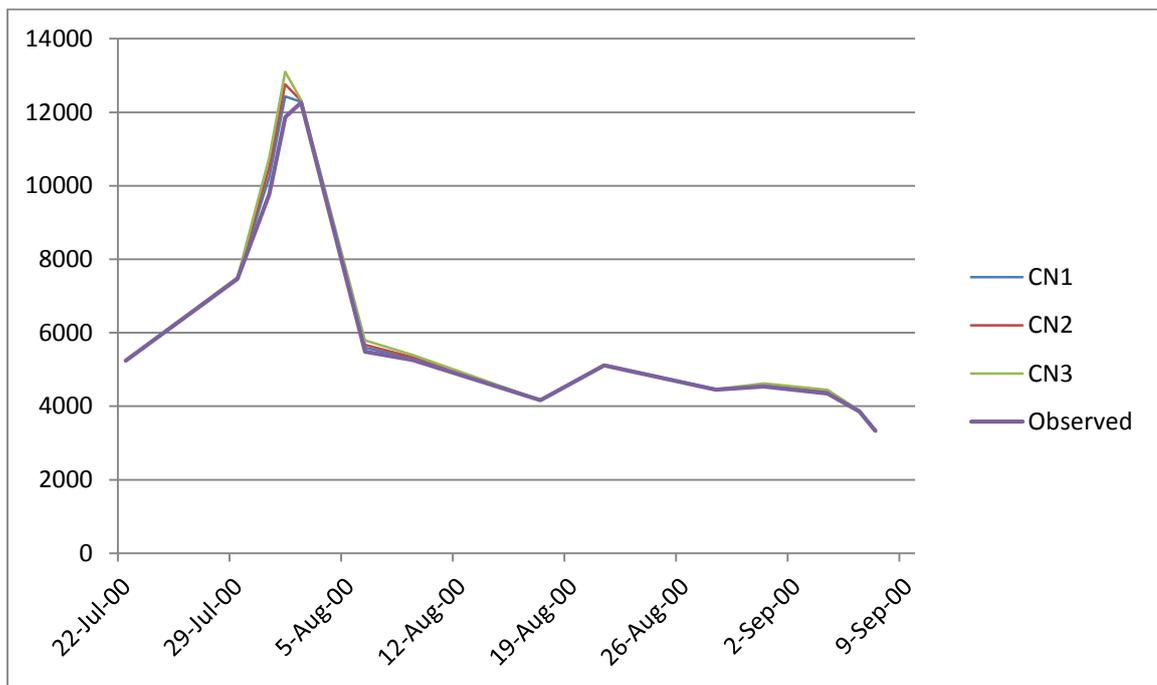


Figure 4.8. Line graph for sensitivity analysis of CN parameter

## 4.7 SENSITIVITY ANALYSIS FOR LULC

Another method was adopted for finding the impact of LULC on the discharge. First the model was simulated with LULC scenario of 2000 and others parameters were set for the simulation; then keeping the same values of other parameters, only the LULC scenario was changed from 2000 to 2010 and simulation was made. LULC impact on the runoff can be examined if the calibrated models are used to run the model for each land use scenario on the same rainfall event and the volume of generated runoff and the resulting stream flows are compared with one another (Lan et al., 2012).

The results were calculated for the runoff simulated from precipitation and there was no base flow involved. Graph of the results for selected events can be as:

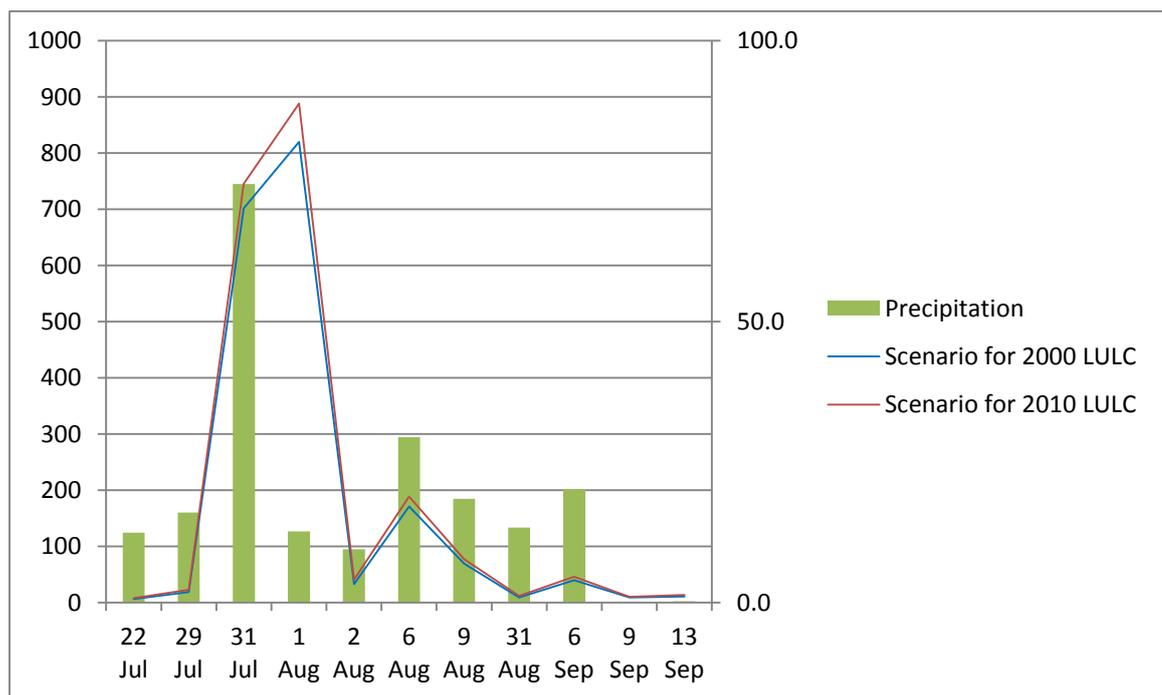


Figure 4.9. Line graph for sensitivity analysis of LULC scenarios of 2000 and 2010. Graph shows that discharge simulated with 2010 LULC is slightly higher than the discharge generated with 2000 LULC scenario. But the difference is negligible overall.

#### **4.8 MANSEHRA CITY SUB-WATERSHED ANALYSIS**

The impact of LULC change on the discharge values was calculated through sensitivity analysis of the whole Tarbela watershed. The results showed that the impact of LULC change was negligible for the whole watershed. These findings were related to the fact that the watershed contains a very small proportion (less than 1%) of the built-up area class in it. Studies showed that the increase or decrease in the discharge of watershed over a period is directly related to the amount of change in the built (impervious area).

To analyze this a small sub-watershed containing a good proportion of built area was extracted from the whole watershed as shown in figure 4.10. This sub-watershed includes a part of the Mansehra city in the Khyber Pakhtunkhwa province of Pakistan. The area of the sub watershed was 16 km<sup>2</sup>. The proportion of built up area in it was 8.2% for the year 2000 and 13.7 % for the year 2010. So there was an increase of 40% in the built area of sub-watershed in 10 years' time.

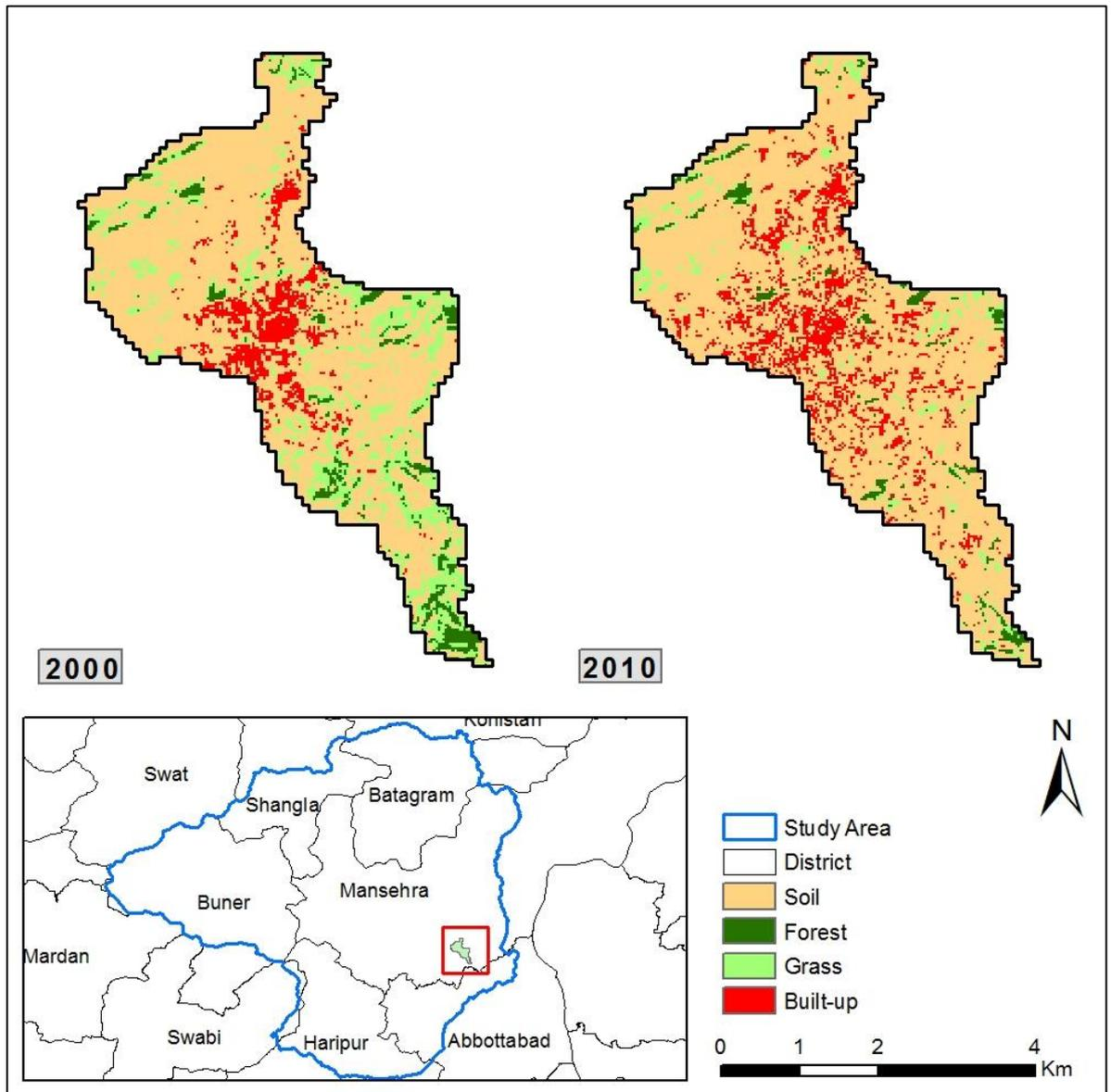


Figure 4.10. LULC of metropolitan sub-watershed in Mansehra District of KP province in Pakistan with a distinct proportion off built-up class in it.

Table 4.6. LULC change of Mansehra subwatershed for the year 2000 and 2010

Class	Area in 2000 (Km <sup>2</sup> )	Percentage of total Area	Area in 2010 (Km <sup>2</sup> )	Percentage of total Area
Soil	11.17	69.53	12.58	78.30
Forest	0.87	5.41	0.52	3.25
Grass	2.71	16.86	0.75	4.69
Built-up	1.32	8.20	2.21	13.76

Model calibrated parameters for the whole watershed were used to simulate the discharge for the smaller watershed. Simulations were made for 8 different events, with precipitation value of more than 15 mm, for each LULC scenario of 2000 and 2010 by just changing the LULC parameter. The results showed a significant percentage of increase in discharge for each event. The simulated results for the whole watershed were then compared with sub-watershed results as shown in table 4.7. The discharge values are in cumecs while the precipitation values (P) are in mm.

Because of the fact the difference in discharge values for a sub-watershed and whole watershed is huge; the percentage change in discharge from the year 2000 to 2010 is calculated. Averaging out the percentage of increase for different events of precipitations it can be concluded that overall the discharge of events in the whole watershed increases by 6.1% from 2000 to 2010, whereas, in a sub-watershed with a good proportion of built-up area in it, the average increase in the discharge values is about 33.6% from 2000 to 2010 as shown in figure 4.11.

Table 4.7. Comparing the percentage increase in discharge values for whole Tarbela watershed and sub-watershed at Mansehra

Date	Rain	Whole watershed			Mansehra City		
		2000 LULC	2010 LULC	Percentage increase	2000 LULC	2010 LULC	Percentage increase
22 Jul	33.98	139.6	150	<b>6.93</b>	1.5	2	<b>25.00</b>
29 Jul	21.45	41.2	44.9	<b>8.24</b>	0.4	0.6	<b>33.33</b>
6 Aug	24.85	176.3	183.9	<b>4.13</b>	0.9	1.2	<b>25.00</b>
9 Aug	15.06	33.8	34.6	<b>2.31</b>	0.3	0.5	<b>40.00</b>
28 Aug	21.00	35.2	38.2	<b>7.85</b>	0.6	0.9	<b>33.33</b>
31 Aug	17.43	24.6	26	<b>5.38</b>	0.3	0.6	<b>50.00</b>
6 Sep	21.56	40.8	44.2	<b>7.69</b>	0.5	0.7	<b>28.57</b>
		Average percentage increase in discharge		<b>6.08</b>	Average percentage increase in discharge		<b>33.61</b>

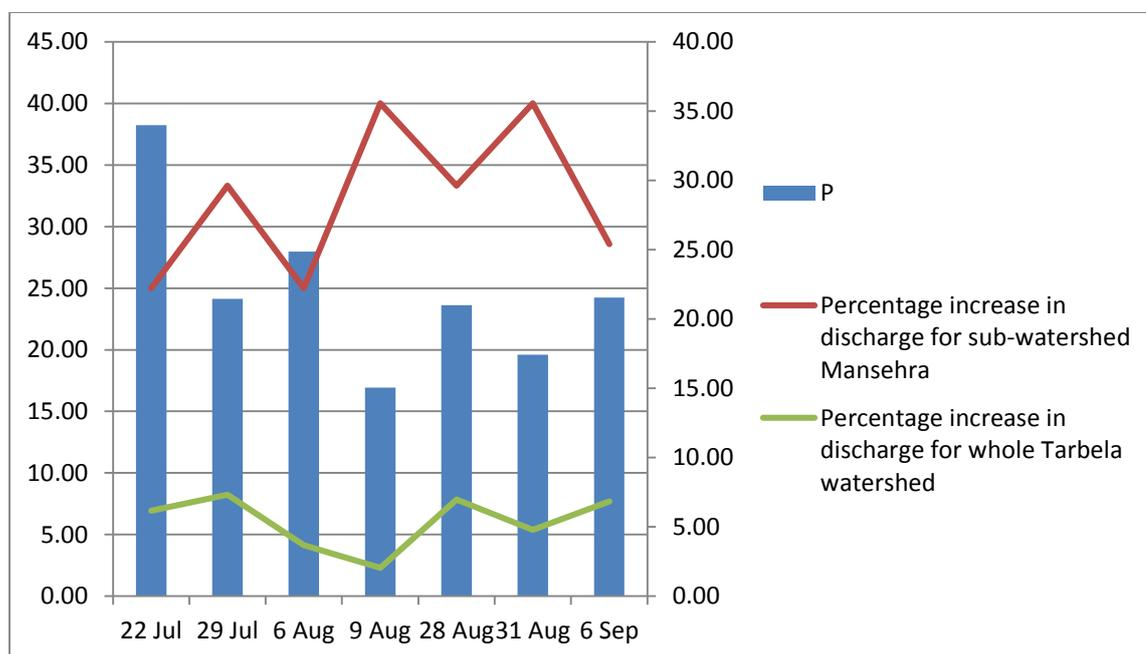


Figure 4.11. Graph showing the difference in percentage increase of discharge for whole Tarbela watershed with less than 1% built area and sub-watershed in Mansehra with about 10% built-up area.

## **CONCLUSIONS AND RECOMMENDATIONS**

### **5.1 CONCLUSION**

The main objective for carrying out this research was to study the impact of LULC on the hydrological response (discharge) of the Tarbela watershed. To carry out the research Landsat imagery was used for analyzing the LULC change for 10 years from 2000-2010. The main land cover in the area are grass land, forest cover and barren soils. The LULC maps generated through supervised image classification shows a change in soil and forest cover in the area.

HEC-HMS hydrological model was used to generate the discharge for the July-September months monsoonal periods of 2000 and 2010. The model was calibrated for the year 2000 using the rainfall data and discharge data. Sensitivity analysis was also done for calibrating the model. Two parameters were found more influencing in determining the overall discharge results; those are curve number values and initial abstraction values.

The validating simulation was done for the year 2010. The simulated discharge from HEC-HMS model was than plotted with the ground observation data at Tarbela. The correlation coefficient of the results is 0.9 for both the calibration and validation scenarios. The relative biasness was calculated as -9% for the 2000 year and -14% for the 2010 year. Although there is a good correlation between simulated and ground observed discharge data, the difference at the peak is quite high for both calibrated and validated year. This is a drawback in the HEC-HMS model.

The effects of LULC on the discharge values were done by sensitivity analysis of the LULC parameter. The model parameters were set for the best calibrated values and only the LULC data was changed. The graph was plotted for the simulations of the two scenarios. From the analysis done through this method, it was observed that changing the factor of LULC alone does not cause any considerable change in the runoff values simulated from the model. So the impact of LULC on hydrology for a large watershed is limited, especially if the watershed does not have considerable built-up area class and the runoff simulation is done with a lumped hydrological model.

In relation to the above generated results of the model, which showed negligible change in discharge because of very small proportion of built-up area in it, the same simulation setup was applied to a very small watershed of 16 km<sup>2</sup> having good proportion of built-up area in it . The model parameters were same as those of the whole watershed. The results showed increased discharge values of about 33% in the smaller watershed in 2010 LULC than in 2000 LULC with increase in built-up area from 8% to 13% (about 40% increase), proving the hypothesis that changes in LULC has its impact on the discharge.

## 5.2 RECOMMENDATIONS

- The distribution of satellite based precipitation data is a utility for getting the distributed results even at sub-basin level. But the problem with lumped model is that it takes into account the whole area and do not analyze the spatial distribution of it. So the simulation done through a distributed model will be helpful in getting a more detailed effect of LULC on the discharge especially in the built up areas. Also the increased number of discharge gauges in the study area will help in calibrating the model to give more precise results.
- Improved temporal analysis can give better results, if the satellite images for each year between 2000 and 2010 can be acquired.
- Improved spatial resolution of soil data will help in calculating the loss and transform more precisely.
- Model simulation for a sub-watershed having more percentage of built-up area (Mansehra Dist.) will help in determining the impacts of LULC change on the area

## REFERENCES

- Abayneh, A. Evaluation of climate change impact on extreme hydrogeological event.
- AghaKouchak, A., Nasrollahi, N., Habib, E., 2009. Accounting for uncertainties of the TRMM satellite estimates. *Remote Sensing* 1, 606 - 619, doi:610.3390/rs1030606
- Akhtar, A. 2013. Indus basin floods: Mechanisms, impacts, and management. Asian Development Bank.
- Ali, K. F., & De Boer, D. H. (2007). Spatial patterns and variation of suspended sediment yield in the upper Indus River basin, northern Pakistan. *Journal of hydrology*, 334(3), 368-387.
- Andréassian, V., Perrin, C., Michel, C., Usart-Sanchez, I., Lavabre, J., 2001. Impact of imperfect rainfall knowledge on the efficiency and the parameters of watershed models. *Journal of Hydrology* 250, 206-223.
- Archer, D. (2003). Contrasting hydrological regimes in the upper Indus Basin. *Journal of Hydrology*, 274(1), 198-210.
- Aronica, G., Hankin, B.G. and Beven, K.J., 1998. Uncertainty and equifinality in calibrating distributed roughness coefficients in a flood propagation model with limited data. *Advances in Water Resources Technology*, 22(4): 349-365.
- Bashar, K. E., & Zaki, A. F. (2005). SMA Based Continuous Hydrologic Simulation of the Blue Nile. In A paper published in the International Conference of UNESCO Flanders FUST FRIEND/NILE Project.
- Bates, P.D., 2004. Remote sensing and flood inundation modeling. *Hydrological Processes*, 18: 2593- 2597.
- Bookhagen, B., & Burbank, D. W. (2010). Toward a complete Himalayan hydrological budget: Spatiotemporal distribution of snowmelt and rainfall and their impact on river discharge. *Journal of Geophysical Research: Earth Surface* (2003–2012), 115(F3).
- Cunderlik, J., & Simonovic, S. P. (2004). Selection of calibration and verification data for the HEC-HMS hydrologic model. Department of Civil and Environmental Engineering, The University of Western Ontario, 10-38.

- Dai, X., & Khorram, S. (1999). A feature-based image registration algorithm using improved chain-code representation combined with invariant moments. *Geoscience and Remote Sensing, IEEE Transactions on*, 37(5), 2351-2362.
- Draper, C.S., Walker, J.P., Steinle, P.J., de Jeu, R.A.M., Holmes, T.R.H., 2009. An evaluation of AMSR-E derived soil moisture over Australia. *Remote Sensing of Environment* 113, 703-710.
- Droogers, P., Bastiaanssen, W., 2002. Irrigation performance using hydrological and remote sensing modeling. *Journal of Irrigation and Drainage Engineering* 128, 11-18.
- Foody, G. M. (2004). Thematic map comparison: evaluating the statistical significance of differences in classification accuracy. *Photogrammetric engineering and remote sensing*, 70(5), 627-634.
- Franchito, S.H., Rao, V.B., Vasques, A.C., Santo, C.M.E., Conforte, J.C., 2009. Validation of TRMM precipitation radar monthly rainfall estimates over Brazil. *Journal of Geophysical Research* 114, D02105.
- Gebremichael, M., Anagnostou, E.N., Bitew, M.M., 2010. Critical steps for continuing advancement of satellite rainfall applications for surface hydrology in the Nile river basin. *Journal of the American Water Resources Association* 46, 361-366
- Hong, Y., Hsu, K.I., Moradkhani, H., Sorooshian, S., 2006. Uncertainty quantification of satellite precipitation estimation and Monte Carlo assessment of the error propagation into hydrologic response. *Water Resources Research* 42, W08421, doi:08410.01029/02005WR004398.
- Hossain, F., Anagnostou, E.N., Bagtzoglou, A.C., 2006. On Latin hypercube sampling for efficient uncertainty estimation of satellite rainfall observations in flood prediction. *Computers & Geosciences* 32, 776-792
- Hossain, F., Huffman, G.J., 2008. Investigating error matrices for satellite rainfall data at hydrologically relevant scales. *Journal of Hydrometeorology* 9, 563-575.
- Immerzeel, W.W., Gaur, A., Zwart, S.J., 2008b. Integrating remote sensing and a process-based hydrological model to evaluate water use and productivity in a south Indian catchment. *Agricultural Water Management* 95, 11-24.
- Jha, A. K., Bloch, R., & Lamond, J. (2012). *Cities and flooding: a guide to integrated urban flood risk management for the 21st century*. World Bank Publications.
- K.D. Beven, *Rainfall-Runoff modeling, The Primer*, Wiley Press, 1999.

- Karssenber, D., 2002. The value of environmental modelling languages for building distributed hydrological models. *Hydrological Processes*, 16: 2751-2766.
- Kurothe, R.S., Goel, N.K. and Mathur, B.S., 2001a. Derivation of a curve number and Kinematicwave based flood frequency distribution. *Hydrological Sciences*, 46(4): 571 – 584
- Lan, A., Wilderman, C., & Richeson, D. (2012). Evaluation of the impact of land use change on stream flow of monocacy creek, northampton county, pa.
- Legates, D. R., & McCabe, G. J. (1999). Evaluating the use of “goodness-of-fit” measures in hydrologic and hydroclimatic model validation. *Water resources research*, 35(1), 233-241.
- Lillesand, T. M., Kiefer, R. W., & Chipman, J. (2000). *Remote sensing and image analysis*. John Wiley and Sons, New York. 820.
- M.R. Knebl, Z.L. Yang, K. Hutchison, and D.R. Maidment, “Regional Scale Flood Modeling using NEXRAD Rainfall, GIS, and HEC-HMS/RAS: A case study for the San Antonio River Basin Summer 2002 storm event,” *Journal of Environmental Management*, vol. 75, pp. 325–336, 2005.
- Maidment, D.R., 1993. GIS and hydrological modelling. In M. F. Goodchild, B. Parks, & L. Steyaert, *Environmental Modelling with GIS* New York, USA. 147-167.
- Maity, D. K. (2009). *Hydrological and 1 D Hydrodynamic Modelling in Manali Sub-Basin of Beas River, Himachal Pradesh, India*.
- Melesse, A. M., & Shih, S. F. (2002). Spatially distributed storm runoff depth estimation using Landsat images and GIS. *Computers and Electronics in Agriculture*, 37(1), 173-183.
- Mishra S.K., Jain M.K., Pandey R.P., Singh V.P., (2003), Evaluation of AMC-dependant SCS-CN-based models using large data of small watersheds, *Water, Energy Int.* vol. 60, no. 3, pp.13–23.
- Mishra S.K., Singh V.P., (2003), *Soil Conservation Service Curve Number (SCS-CN) Methodology*, Kluwer Academic Publishers, Dordrecht, Netherland
- Owojori, A., & Xie, H. (2005, March). Landsat image-based LULC changes of San Antonio, Texas using advanced atmospheric correction and object-oriented image analysis approaches. In *5th International Symposium on Remote Sensing of Urban Areas*, Tempe, AZ.

- Pappenberger, F., Beven, K.J., Ratto, M. and Matgen, P., 2008. Multi-Method Global Sensitivity Analysis of Flood Inundation Models. *Advance in Water Resources*, 31: 1-14.
- Rahman, A., Lee, H. K., & Khan, M. A. (1997). Domestic water contamination in rapidly growing megacities of Asia: Case of Karachi, Pakistan. *Environmental Monitoring and Assessment*, 44(1-3), 339-360.
- Sabins, F. F. (1999). Remote sensing for mineral exploration. *Ore Geology Reviews*, 14(3), 157-183.
- Shrestha, M. S., Artan, G. A., Bajracharya, S. R., & Sharma, R. R. (2008). Using satellite-based rainfall estimates for streamflow modelling: Bagmati Basin. *Journal of Flood Risk Management*, 1(2), 89-99.
- Stevens, M. (2012). *Cities and Flooding: A Guide to Integrated Urban Flood Risk Management for the 21st Century* by Abhas Jha, Robin Bloch, Jessica Lamond, and other contributors.
- Tahir, A. A., Chevallier, P., Arnaud, Y., Neppel, L., & Ahmad, B. (2011). Modeling snowmelt-runoff under climate scenarios in the Hunza River basin, Karakoram Range, Northern Pakistan. *Journal of Hydrology*, 409(1), 104-117.
- Thomas, M. L., Ralph, W. K., & Chipman, J. W. (2000). *Remote sensing and image interpretation*. John Wiley and sons, Newyork. 763.
- Tobin, K. J., & Bennett, M. E. (2010). Adjusting satellite precipitation data to facilitate hydrologic modeling. *Journal of Hydrometeorology*, 11(4), 966-978.
- USDA, S. (1986). *Urban hydrology for small watersheds*. Technical release, 55, 2-6.
- Van Loon, L.R. and Jakob, A., 2005. Evidence for a second transport porosity for the diffusion of tritiated water (HTO) in a sedimentary rock (Opalinus Clay - OPA): application of throughand out-diffusion techniques. *Transport in Porous Media*, 61(2): 193-214.
- Winsemius, H.C., Savenije, H.H.G., Bastiaanssen, W.G.M., 2008. Constraining model parameters on remotely sensed evaporation: justification for distribution in ungauged basins? *Hydrology and Earth System Sciences* 12, 1403-1413.
- Wipfler, E.L., Metselaar, K., van Dam, J.C., Feddes, R.A., van Meijgaard, E., van Ulft, L.H., van den Hurk, B., Zwart, S.J., Bastiaanssen, W.G.M., 2011. Seasonal evaluation of the land surface scheme HTESSEL against remote sensing derived energy fluxes of the Transdanubian region in Hungary. *Hydrology and Earth System Sciences* 15, 1257-1271.

- Yilmaz, K. K., Hogue, T. S., Hsu, K. L., Sorooshian, S., Gupta, H. V., & Wagener, T. (2005). Intercomparison of rain gauge, radar, and satellite-based precipitation estimates with emphasis on hydrologic forecasting. *Journal of Hydrometeorology*, 6(4).
- Zhou, T., Yu, R., Chen, H., Dai, A., & Pan, Y. (2008). Summer precipitation frequency, intensity, and diurnal cycle over China: A comparison of satellite data with rain gauge observations. *Journal of Climate*, 21(16).